



Pontificia Universidad Católica del Perú

Escuela de Posgrado

**Optimal Design of a Photovoltaic Station Using Markov and
Energy Price Modelling**

**Tesis para obtener el grado académico de Magíster en Ingeniería
Mecatrónica**

Presentado por: Ing. Marcio Boris Salazar Márquez

Tutor Responsable (TU Ilmenau) : Dr. Ing. Aouss Gabash
Professor Responsable (TU Ilmenau) : Prof. Dr. Yuri Andri Shardt Wolchuk
Professor Responsable (PUCP) : Prof. Dr. Ing. Julio César Tafur Sotelo

Abril, 2023


Informe de Similitud

Yo, Julio César Tafur Sotelo, docente de la Escuela de Posgrado de la Pontificia Universidad Católica del Perú, asesor de la tesis de investigación titulado optimal Design of a Photovoltaic Station Using Markov and Energy Price Modelling, del autor Marcio Boris Salazar Márquez dejo constancia de lo siguiente:

- El mencionado documento tiene un índice de puntuación de similitud de 34%. Así lo consigna el reporte de similitud emitido por el software *Turnitin* el 04/04/2023.
- He revisado con detalle dicho reporte y la Tesis y no se advierte indicios de plagio.
- Las citas a otros autores y sus respectivas referencias cumplen con las pautas académicas.

Lugar y fecha:

Lima, 17/04/2023

Apellidos y nombres del asesor: Tafur Sotelo, Julio César Paterno Materno, Nombre1 Nombre 2	
DNI: 06470028	
ORCID: 0000-0003-3415-1969	
Firma	

Master's Topic Proposal

for Marcio Boris Salazar Marquez

Title: Optimal Design of a Photovoltaic Station Using Markov and Energy Price Modelling

Note a master's thesis requires a time commitment of 750 h.

Background: Due to environmental concerns and fuel cost, large-scale photovoltaic (PV) stations are widespread [1]. Basically, a PV station consists of two parts: 1) PV panels to produce direct current, and 2) PV inverters to convert direct current to alternating current [2]. Given the required dimension of a PV station, that is, the installed peak power of PV panels, a PV station can be optimally designed [2]. In [2], a design method has been proposed to find the optimal number of PV panels and PV inverters, and the final topology of a PV station, while minimizing the levelized cost of the generated electricity. Another design method [3] has considered the reliability of the PV inverters using Markov modelling and the stochastic transitional probability matrix [4]. In this project, a new optimal design method will be developed using both Markov [3] and energy price modelling [2], while exploring the profitability [5] of a PV station with an installed peak power up to 100 kWp. The data (four samples per hour for one year, that is, 35,040 sample) of the injected energy from a reference PV station in Germany will be made available.

Project Description:

Development of an optimal design method for planning a PV station using combined Markov [3][4] and energy price modelling [2][5].

Thesis Objectives:

- 1) Literature review of optimization methods for designing PV stations;
- 2) Develop a new optimal design method using Markov and energy price modelling, while considering the operational constraints of the PV panels and the PV inverters, for example, the power rating, the operating voltage, and current range etc.;
- 3) Apply the developed method to design a PV station and study the profitability of the station designed taking into consideration current prices and technology.

Thesis Output:

1) The written work; 2) Implementation of the new optimal design method and evaluation of the results in MATLAB; and 3) Defence slides.

Literature:

- [1] P. Gevorkian, *Large-Scale Solar Power System Design: An Engineering Guide for Grid-Connected Solar Power Generation*, McGraw Hill Companies, 2011.
- [2] T. Kerekes, E. Koutroulis, D. Sera, R. Teodorescu and M. Katsanevakis, "An optimization method for designing large PV plants", *IEEE J. Photovoltaics*, vol. 3, no. 2, pp. 814-822, Apr. 2013.
- [3] Z. Moradi-Shahrabak, A. Tabesh, and G. R. Yousefi, "Economical design of utility-scale photovoltaic power plants with optimum availability", *IEEE Trans. Ind. Electron.*, vol. 61, no. 7, pp. 3399-3406, July 2014.
- [4] R. Billinton and R. Allan, *Reliability Evaluation of Engineering Systems—Concepts and Techniques*. New York, NY, USA: Plenum Press, 1992.
- [5] M. R. Lindeburg, *Engineering Economic Analysis: An Introduction*. Professional Publications, Inc, USA: Plenum Press, 2001.

Start Date: April 1st, 2022

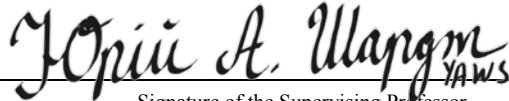
Supervising Professor: Prof. Dr. Yuri A.W. Shardt

Direct Supervisor: Dr.-Ing. Aouss Gabash

Supervisor at PUCP/Lima: Prof. Dr.-Ing. Julio César Tafur Sotelo

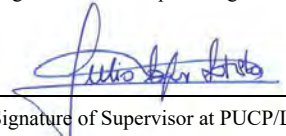
Erfurt, 2022/03/23

City, Date


Signature of the Supervising Professor

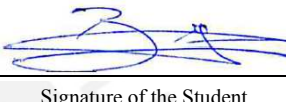
Lima, 2022/03/29

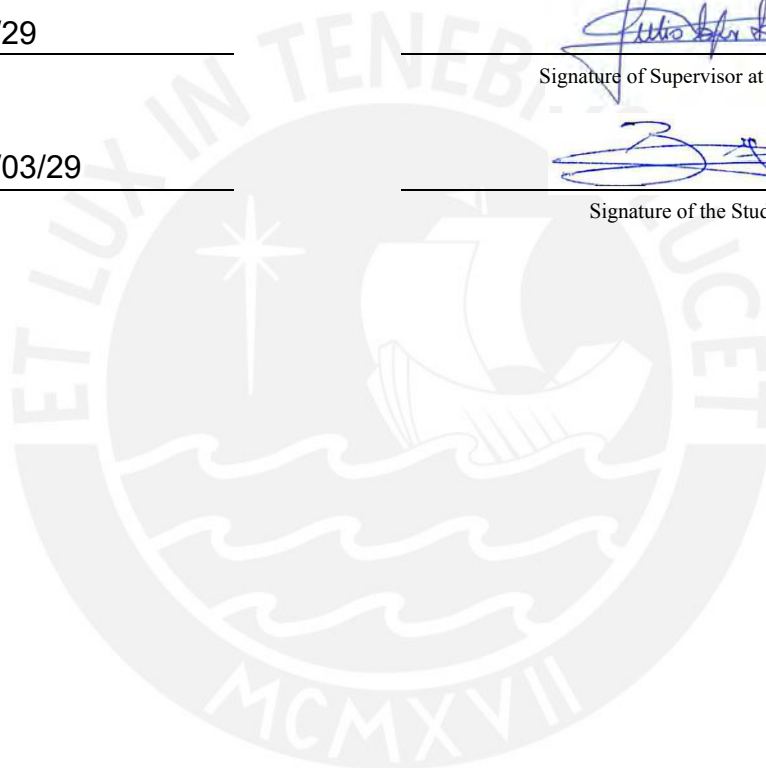
City, Date


Signature of Supervisor at PUCP/Lima

Ilmenau, 2022/03/29

City, Date


Signature of the Student



Selbständigkeitserklärung


Honour Statement

Ich erkläre hiermit, daß ich die vorliegende Arbeit selbständig verfaßt und keine anderen als die angegebenen Quellen benutzt habe. Alle Gedanken, die aus fremden Quellen direkt oder indirekt übernommenen wurden, sind als solche kenntlich gemacht. Die Arbeit wurde bisher keiner anderen Prüfungsbehörde vorgelegt und auch noch nicht veröffentlicht.

I hereby declare that I have written this thesis independently and have not used any other sources than those specified. All thoughts that have been taken either directly or indirectly from other sources have been explicitly identified as such. This thesis has not been submitted for credit in any other degree programme or institution nor has it been previously published.

Ilmenau, 01.11.2022

Ort, Datum | City, Date



Unterschrift | Signature

Abstract

As the fight against anthropogenic global warming increases, photovoltaic (PV) systems, which are a type of renewable energy, are increasingly being considered. In order to use PV systems, it is necessary to develop methods to optimize their configuration, that is, the optimal number of PV modules and inverters. The objectives are to examine the optimization of PVs subject to not only the operational constraints but also the failure and repair events of PV inverters up to 100 kW, while minimizing the effective levelized cost of energy. To achieve this, using Markov modelling, a new energy price model that considers the current prices of the PV inverters is developed as part of a new optimization framework. A case study considering six real PV inverters is developed to show the effectiveness of the framework. In addition, real data from a reference PV station in Germany is used to calculate the average hours per day that a panel generates its rated power to consider the geographical location, temperature and number of sunny days in the given region. Unlike previous work, local and global optimal solutions are found using PV inverters in the range of 15 kW to 100 kW. Therefore, the new findings of this study will be considered in the future, for example, when considering the failure and repair events of PV modules.

Zusammenfassung

Im Rahmen des Kampfes gegen die anthropogene Erderwärmung werden zunehmend Photovoltaikanlagen (PV-Anlagen) in Betracht gezogen, welche zu den erneuerbaren Energien zählen. Um PV-Anlagen nutzen zu können, müssen Methoden zur Optimierung ihrer Konfiguration, d. h. der optimalen Anzahl von PV-Modulen und Wechselrichtern, entwickelt werden. Ziel dieser Arbeit ist es, die Optimierung von PV-Anlagen zu untersuchen, wobei nicht nur die betrieblichen Randbedingungen, sondern auch die Ausfall- und Reparaturereignisse von PV-Wechselrichtern bis zu 100 kW berücksichtigt werden, um dabei die effektiven Stromgestehungskosten zu minimieren. Um dies zu erreichen, wird ein neues Energiepreismodell entwickelt, das die aktuellen Preise der PV-Wechselrichter, sowie die Markoff-Modellierung als Teil eines neuen Optimierungsrahmens berücksichtigt. Anhand einer Fallstudie unter Berücksichtigung von sechs realen PV-Wechselrichtern wird die Wirksamkeit des Rahmens aufgezeigt. Außerdem werden reale Daten einer Referenz-PV-Anlage in Deutschland verwendet, um die durchschnittlichen Stunden pro Tag zu berechnen, in denen ein Modul seine Nennleistung erzeugt. Dazu werden die geografische Lage, die Temperatur und die Anzahl der Sonnentage in der jeweiligen Region berücksichtigt. Im Gegensatz zu früheren Arbeiten werden lokal und global optimale Lösungen mit PV-Wechselrichtern im Bereich von 15 kW bis 100 kW gefunden. Daher können die neuen Erkenntnisse dieser Studie in Zukunft beispielsweise bei der Betrachtung von Ausfall- und Reparaturereignissen von PV-Modulen berücksichtigt werden.

Resumen

Ante la creciente lucha contra el calentamiento global antropogénico, los sistemas fotovoltaicos, que son un tipo de energía renovable, están siendo cada vez más considerados. Para usar sistemas fotovoltaicos, es necesario desarrollar métodos para optimizar su configuración, es decir, el número óptimo de módulos e inversores fotovoltaicos. Los objetivos de esta tesis son examinar la optimización de los sistemas fotovoltaicos sujetos, no sólo a las restricciones operativas, sino también a los eventos de falla y reparación de los inversores fotovoltaicos de hasta 100 kW, mientras se minimiza el costo efectivo nivelado de la energía. Para lograrlo, empleando el modelo de Márkov, se desarrolla un nuevo modelo del precio de la energía que considera los costos actuales de los inversores fotovoltaicos como parte de un nuevo esquema de optimización. Se desarrolla un caso de estudio considerando seis inversores fotovoltaicos reales para mostrar la efectividad del esquema. Asimismo, se utilizan datos reales de una estación fotovoltaica de referencia en Alemania para calcular el promedio de horas al día en que un panel genera su potencia nominal teniendo en cuenta la ubicación geográfica, la temperatura y el número de días soleados de la región. A diferencia de trabajos anteriores, se encuentran soluciones locales y globales óptimas empleando inversores fotovoltaicos en el rango de 15 kW a 100 kW. Por lo tanto, los nuevos hallazgos de este estudio se tomarán en cuenta en el futuro, por ejemplo, cuando se contemplen los eventos de falla y reparación de los módulos fotovoltaicos.

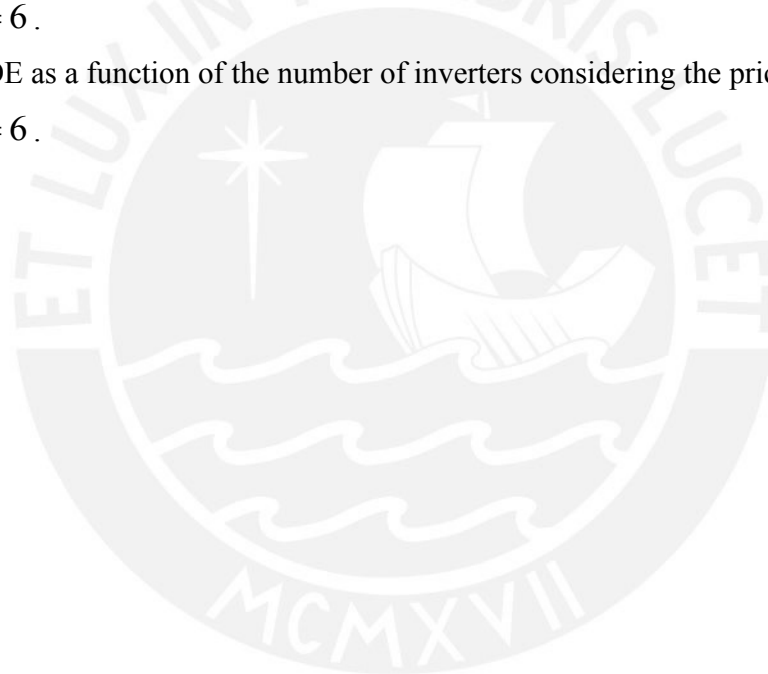
Contents

Chapter 1 : Introduction	1
1.1 Problem Statement and Motivation	1
1.2 Contributions and Master's Thesis Structure	2
1.3 Software for Optimization	3
Chapter 2 : State of the Art	4
2.1 Sustainable Energy	4
2.2 Photovoltaic Systems	7
2.3 Modelling of a Photovoltaic Station	12
2.4 Optimal Design Methods for Photovoltaic Stations	13
2.5 Operational Constraints	19
Chapter 3 : Optimal Design Method	23
3.1 Markov Modelling	23
3.2 Energy Price Modelling	27
3.3 Proposed Optimal Design Method	29
Chapter 4 : Results	38
4.1 System Description	38
4.2 Results and Discussion	40
Chapter 5 : Conclusions and Future Work	49
5.1 Conclusions	49
5.2 Future Work	49
References	50
Appendix I : MATLAB Code	55
I.1 Sub-Code 1: Energy Price Modelling	55
I.2 Sub-Code 2: Markov Modelling	56

List of Figures

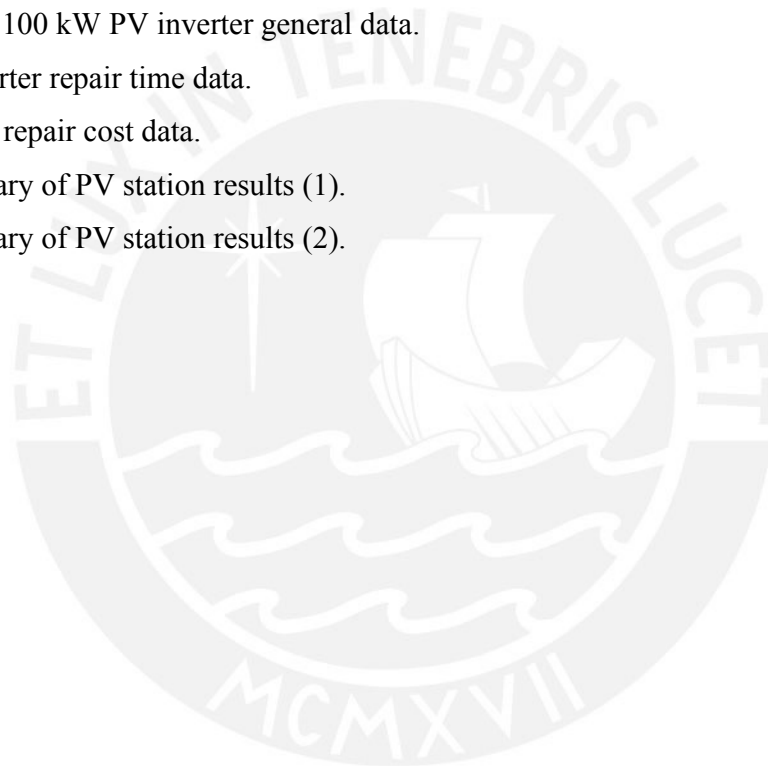
Figure 1: Capacity of PV installations (GW) due to the Inflation Reduction Act (IRA).	1
Figure 2: Global fossil CO ₂ emissions in 2021.	4
Figure 3: Net renewable capacity additions, 2011-2022.	5
Figure 4: The trend of the LCOE of renewable systems since 2010 to 2019.	7
Figure 5: Types of PV modules: (a) Monocrystalline, (b) Polycrystalline, (c) Thin-film.	8
Figure 6: Stand-alone PV system.	10
Figure 7: Grid-connected PV system.	10
Figure 8: Bimodal PV system.	10
Figure 9: Residential PV system.	11
Figure 10: Commercial PV system.	11
Figure 11: Utility-scale PV system.	12
Figure 12: Block diagram of a generalized PV station.	13
Figure 13: Arrangement of PV set.	14
Figure 14: Arrangement of PV sets in blocks.	15
Figure 15: Arrangement and orientation of PV sets in the available installation area.	15
Figure 16: Basic topologies for PV stations: (a) Centralized, (b) string, (c) multistring, and (d) AC modular.	16
Figure 17: Circuit diagram of Huawei 100 kW PV inverter interconnection.	22
Figure 18: Huawei 100 kW PV inverter.	22
Figure 19: Example of two-state Markov chain.	23
Figure 20: Tree diagram of two-state system.	24
Figure 21: Markov model states and transitions of a PV system.	25
Figure 22: two-state system transient behavior.	26
Figure 23: Five-state system transient behavior.	26
Figure 24: New energy price model flow diagram.	27
Figure 25: Cost of PV inverters versus inverter size.	28
Figure 26: The real data of the injected energy is available from a reference PV station in Langewiesen, Germany.	29
Figure 27: Flowchart for optimal design.	37

Figure 28: Configuration of a PV station with $n_i = 1$.	38
Figure 29: Configuration of a PV station with $n_i = 5$.	39
Figure 30: The inverter size as a function of the number of inverters.	41
Figure 31: Failure rate (λ) as a function of the inverter size.	42
Figure 32: Repair rate (μ) as a function of the inverter size.	43
Figure 33: NSEE as a function of the inverter size.	44
Figure 34: ELCOE as a function of the number of inverters considering the prices in 2022.	45
Figure 35: ELCOE as a function of the number of inverters considering the prices in 2012.	46
Figure 36: ELCOE as a function of the number of inverters considering the prices in 2012 and $h = 6$.	47
Figure 37: ELCOE as a function of the number of inverters considering the prices in 2022 and $h = 6$.	48



List of Tables

Table 1: PV module electrical data at Standard Test Conditions.	19
Table 2: PV module electrical data at Nominal Operating Cell Temperature.	19
Table 3: PV module mechanical characteristics.	20
Table 4: Huawei 100 kW PV inverter efficiency specifications.	20
Table 5: Huawei 100 kW PV inverter input specifications.	20
Table 6: Huawei 100 kW PV inverter output specifications.	21
Table 7: Huawei 100 kW PV inverter general data.	21
Table 8: PV inverter repair time data.	33
Table 9: Inverter repair cost data.	36
Table 10: Summary of PV station results (1).	40
Table 11: Summary of PV station results (2).	40



Nomenclature

A	PV inverters stochastic transitional probability matrix (STM).
c_0, c_1, c_2	PV price factors.
$C_{1kW.2012}, C_{1kW.2022}$	Cost of 1 kW PV inverter in 2012 and in 2022, respectively.
C_1, C_2	PV inverters cost function in 2012 and in 2022, respectively.
$C_{init.2022}$	Initial price factor of 1kW PV inverter 2022.
$C_{i(inv)}$	The initial cost of PV inverters.
C_i	The initial investment cost of a PV power plant.
C_{tr}	The depreciation tax benefit of a PV power plant.
C_y	The total annual cost of a PV power plant.
C_{rv}	The benefit related to the system residual value of a PV power
$C_{t(inv)}$	Total inverter cost during the lifetime of the PV energy system.
$C_{r(inv)}$	The estimation of repair or replacement costs of inverters in a year.
D_1	The length of the southern side of the actual installation area.
DIM_1	The southern dimension of the total available installation area.
D_2	The western dimension of the actual installation area.
DIM_2	The western dimension of the total available installation area.
ELCOE	Effective levelized cost of energy.
E_{tot}	The total generated energy over the physical lifetime of the PV
$E_{y(eff)}$	The amount of effective generated energy in a year.
F_y	The distance required between adjacent PV blocks.
h	The average hours per day that a PV module generates its rated
H_1	The maximum height of a PV module.
H_T	The maximum height of each PV set.
i, j	Indices of PV inverters STM.

$IGEY$	The ideal amount of generated energy in a year.
k	State index of Markov model.
k_e	The efficiency factor due to the losses of the PV modules and the system connections.
LCOE	Levelized cost of energy.
L_{pv1}, L_{pv2}	Length and width of each PV module, respectively.
MPPT	Maximum power point tracking.
MTBF	PV inverters mean time between failures.
MTTR	PV inverters mean time to repair.
$n_{i,max}$	The maximum number of PV inverters.
n_i	Number of PV inverters.
n_s	Number of PV inverters connected in series.
n_p	Number of PV inverters connected in parallel.
N	The lifetime of the PV system in years.
N_r	Number of rows or PV panels.
N_D	The number of days per year.
N_H	The number of hours per day.
p_k	The probability of being in state k of Markov model.
P	the state probability vector of Markov model.
P_{tot}	The installed peak power of PV panels.
PV_{factor}	PV power plant factor.
P_{real}	The real sum of the PV modules generated in a year.
P_{ideal}	The ideal sum of the PV modules generated in a year.
P_{PV}	The rated power of a PV module.
$P_{max}, V_{max}, I_{max}$	The maximum power, voltage and current of a PV set, respectively.
P_{loss}	The inverter power loss.

$R_{\theta_{ja}}$	The thermal resistance between the junction and ambient.
$TGEY$	The total amount of generated energy in a year.
T_j	The transistor junction temperature.
T_a	The maximum ambient temperature in °C
T_d	PV inverter time to repair.
T_{d_k}	The downtime of the $(k - 1)$ faulty PV inverters.
$V_{i,max}$	The PV inverter DC input maximum MPP voltage.
V_{PV}	The rated voltage of PV modules in a PV power plant.
$V_{DC,max}$	PV inverter maximum permissible DC input voltage.
$V_{oc,max}$	PV module maximum open-circuit voltage.
V_x	DC-side voltage of the PV inverter.
w	The wage for skilled workers during the downtime.
W_1	Width of the area of a PV module.
W_T	Width of the area occupied of each PV set.
x	PV inverter size.
x_{max}	Maximum PV inverter size.
$\alpha_1, \alpha_2, \alpha_3, \alpha_4$	Parameters of PV inverters cost function.
β	PV modules tilt angle.
λ	PV inverter failure rate.
$\lambda_b, \pi_A, \pi_E, \pi_Q, \pi_T$	The base failure rate, application factor, the operation environment factor, the quality factor and the temperature factor, respectively.
η	The efficiency of the PV power system.
η_c, η_i	The efficiency of cabling and the PV inverters with PV panels, respectively.
μ	PV inverter repair rate.
rr	The repair cost of PV inverters.

Chapter 1: Introduction

1.1 Problem Statement and Motivation

Renewable energy systems, such as photovoltaic (PV) technologies, are increasingly being considered as an alternative solution to the actual energy demand. Due to the current situation with world pollution and the lack of conventional fuels, governments around the world are passing laws that encourage companies to invest in PV systems [1]. Figure 1 shows the increase in Gigawatt (GW) capacity of PV installations over the next 5 years due to the Inflation Reduction Act (IRA) in the U.S. [1].

A PV station or PV plant consists of basically two parts: 1) PV panels that produce direct current (DC), and 2) PV inverters that convert direct current to alternating current (AC). The type of PV inverters and the way of interconnection has a great effect on the characteristics of the PV station in terms of efficiency, investment cost, reliability of power generation [2]. The PV station can have different topologies, that is, depending on the number of panels and PV inverters. The PV station are classified into four basic groups depending on how the PV modules are interconnected to the PV inverters [2].

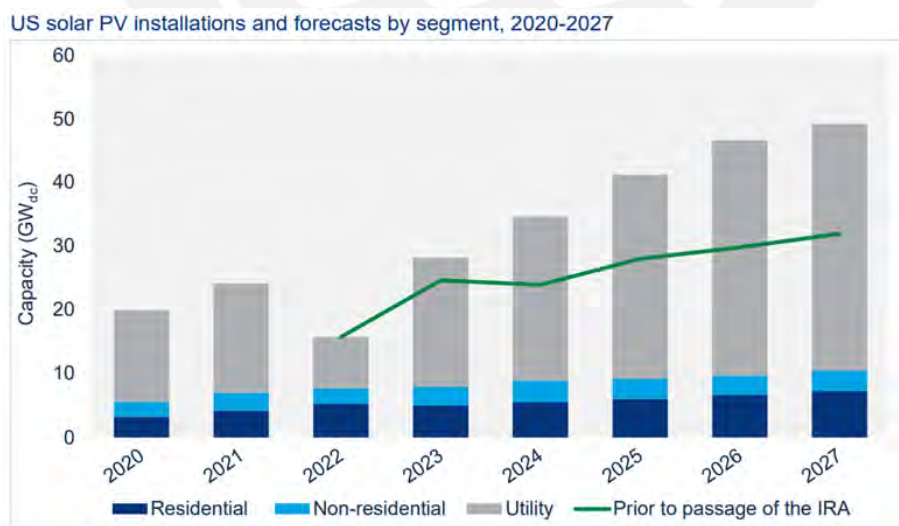


Figure 1: Capacity of PV installations (GW) due to the Inflation Reduction Act (IRA).

The levelized cost of energy (LCOE) is the price that the energy generated must have to balance with the total cost of the plant during its lifetime. The LCOE is also used to make economical comparisons of renewable energy plants with other types of power systems [3]. Furthermore, the effective levelized cost of energy (ELCOE) is presented as a new price modelling that improves the conventional LCOE and includes evaluations of the economic availability of the power plant [2].

Another design method that is considered to evaluate the reliability of PV inverters is Markov modelling [2] [4] [5]. This method evaluates the probabilities of occurrence of PV inverter failure and repair events through state transitions. The stochastic transitional probability matrix (STPM) represents all the transition possibilities in the Markov model. Another consideration in the evaluation of PV station availability is the calculation of the not supplied expected energy (NSEE). The NSEE depends on the size of the PV plant, the Markov model and weather characteristics such as the sunshine time in the region.

In this work, a new optimal design method will be developed using both Markov and energy price modelling of a real PV station with an installed peak power equal to 86-kilowatt peak (kWp). The data (four samples per hour for one year, that is, 35,040 sample) of the injected energy from that station is made available.

1.2 Contributions and Master's Thesis Structure

The contributions of this Master's Thesis can be summarized as follows:

- Based on [2], a new method is developed to determine the time that PV panels generate power during a year, so that the effects of the geographical location, temperature and number of sunny days in the region can be considered.
- A new price model is developed in order to consider current prices of PV inverters in 2022.
- A framework combining both Markov and the new price model is introduced to find the optimal design of a PV station.
- Real data of 6 sizes of PV inverters are used in the design process and the results are compared with previous works to show the effects of the new energy price modelling.

Chapter 2 gives a short review of conventional and sustainable energy sources. Since the main focus in this work is on presenting a method for the optimal design of a PV station, a detail review of the configurations is given for such PV systems. In addition, the Markov and energy price modelling as a method used for designing an optimal PV station is reviewed. Finally, the operational constraints of the PV components are presented.

In Chapter 3 the proposed optimal method in the design of the PV station is developed by evaluating the reliability of the plant with Markov and the new energy price modelling.

Chapter 4 shows the summary of the results obtained using the new design method. The most important parameters are analysed and compared with different scenarios. A discussion is made on the basis of the results.

Finally, final conclusions and future work that remains to be investigated in this project are presented in Chapter 5.

1.3 Software for Optimization

The problem in this work is formulated as a mixed integer nonlinear optimal design problem, in which not only operational constraints, but also design constraints have to be satisfied. The model equations developed in this work are implemented as an optimization framework. The numerical computations and the solution algorithms are implemented in MATLAB R2021b [6], where sub-codes for energy price and Markov modelling are given in the appendix.

Chapter 2: State of the Art

2.1 Sustainable Energy

The term sustainable energy, unlike other types of more polluting and expensive conventional energy, is a form of energy that is obtained through natural and inexhaustible sources and is called renewable energy sources, that is, as through the sun, rain, the movement of water such as rivers and seas, etc. An energy is sustainable if current energy needs are satisfied without compromising future generations [7].

In [8] the global energy problem is presented as a consequence of the use of conventional energy sources that produce more greenhouse gas emissions and also the problem of energy access. Conventional or non-renewable energy sources are those that are of limited quantity in nature and are grouped into two categories according to their extraction, fossil fuels and nuclear power.

Fossil fuels are materials containing hydrocarbons (carbon and hydrogen) formed naturally in the earth's crust from the remains of dead animals and plants, which are extracted and burned for fuel to produce energy. The main types of fossil fuels are coal, crude oil and natural gas, and are some of the most important natural resources that we use every day [9]. However, the use of fossil fuels produces a large amount of carbon dioxide (CO₂) emissions each year, which is harmful to the environment. Figure 2 shows the global fossil CO₂ emissions in 2021 where despite a 5.4% drop in emissions in 2020 due to COVID-19, in 2021 CO₂ emissions increased again by almost 5% [10].

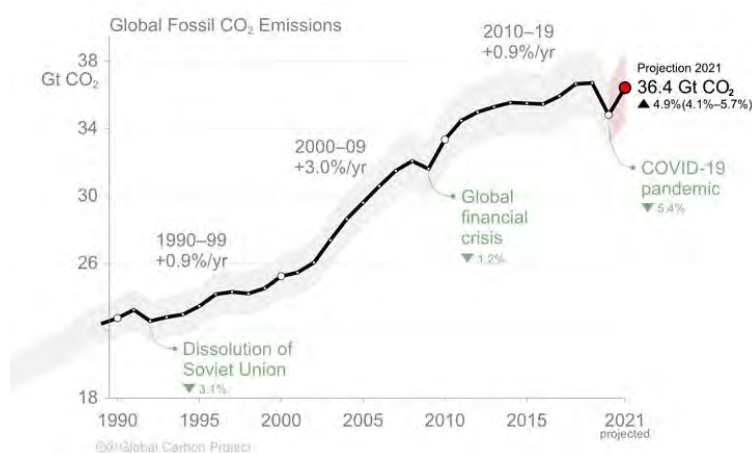


Figure 2: Global fossil CO₂ emissions in 2021.

Nuclear power is also a form of energy obtained through atomic reactions to produce electrical, thermal and mechanical energy. In the European Union, one third of the electrical energy is produced by nuclear power plants [11]. However, the cost of installing and maintaining a nuclear power plant is becoming increasingly expensive and there is also a high risk of contamination in the event of an accident. Similar to fossil fuels, nuclear energy produces high levels of CO₂ emissions [12].

Renewable energy sources are playing an increasingly important role in power generation and, despite the challenges of supply chain shortages caused by the pandemic, new additions in renewable capacity increased by more than 45% in 2019 and the trend is estimated to continue in the coming years [13]. Figure 3 shows the net renewable capacity additions from 2011 to 2022, where the increase in capacity is expected to be almost 280 Gigawatt (GW) in 2022 [13].

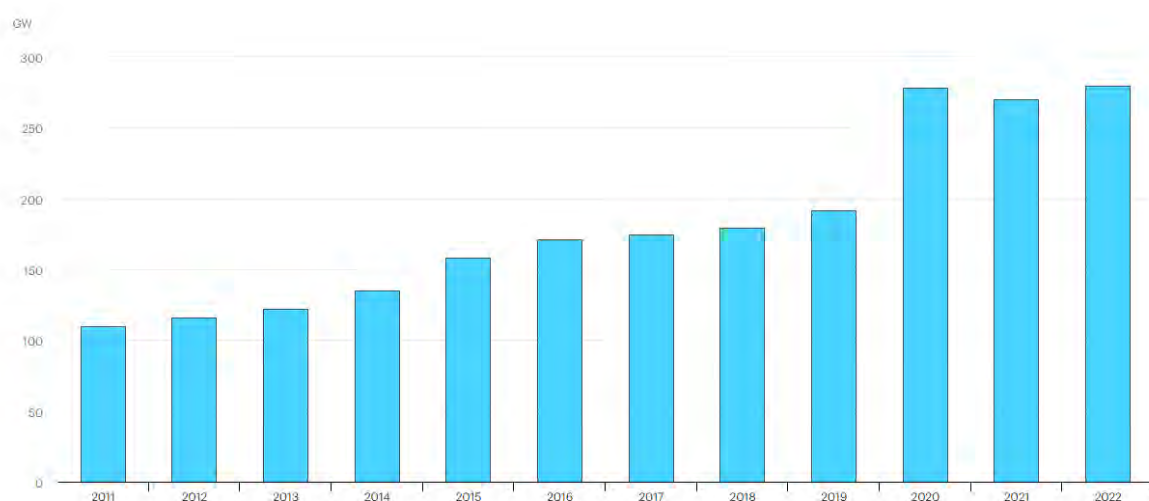


Figure 3: Net renewable capacity additions, 2011-2022.

Around 257 GW were added worldwide in 2021, increasing the stock of renewable power by 9.1% compared to the previous year [14]. The main renewable energy sources are: hydropower, solar energy, wind power, geothermal and bioenergy. Hydropower is the renewable source with the largest energy capacity, producing around 1360 GW in 2021 which represents an addition of 25 GW with respect to 2020. However, solar and wind power have higher year-over-year increases in renewable additions. Solar energy alone accounted for more than half in renewable additions with 133 GW in 2021 and wind power with 93 GW [14].

Solar energy systems use radiant light and heat from the sun to generate electric energy or electricity [15]. The main solar energy technologies are PV systems, solar heating, concentrated solar power (CSP) and artificial photosynthesis [16]. PV systems convert sunlight into electricity by using semiconductor materials through the photovoltaic effect. For this, PV panels are used to generate light into electric energy and PV inverters that transform the energy produced by the panels into usable energy [15]. Solar heating accumulates heat by absorbing sunlight through energy collectors, which are devices for heating water or air [17]. CPS systems use a mirror configuration to concentrate the light from the sun into a receiver and convert it into heat, then the heat can be used to drive a turbine to generate electricity or use the heat for industrial processes [18]. Artificial photosynthesis technology consists of imitating the natural effect of photosynthesis, in which sunlight is captured and this energy is used to chemically convert water and carbon dioxide into fuels [16].

Wind power, as mentioned above, is another type of renewable energy with more additions and consists of harnessing the air flow to run wind turbines to generate electricity [14]. Worldwide, about 1,700 Terawatt (TW) were generated in 2021, representing approximately 2% of the world's energy [14].

Geothermal energy is thermal energy found in the earth's crust and originated from the formation of the planet and the radioactive decay of materials [19]. The heat is used to produce electricity or also for use in steam boilers. Around 15 GW has been generated globally by 2021 [14].

Bioenergy is a source of energy obtained by burning biomass fuel. Biomass comes from organic residues such as plants and animals. Fossil fuels also come from organic residues; however, the difference with biomass is that it takes carbon from the atmosphere as it grows and gives back what is burned, making it a sustainable form of energy, while fossil fuels require many years of decomposition to be used [20].

In summary, renewable systems are becoming more relevant today as alternative sources of energy and at increasingly lower installation costs. Figure 4 shows the trend of the levelized cost of energy (LCOE) of renewable systems since 2010 to 2019 and PV systems presented the largest decline in LCOE as we increased capacity [12].

Electricity from renewables became cheaper as we increased capacity – electricity from nuclear and coal did not

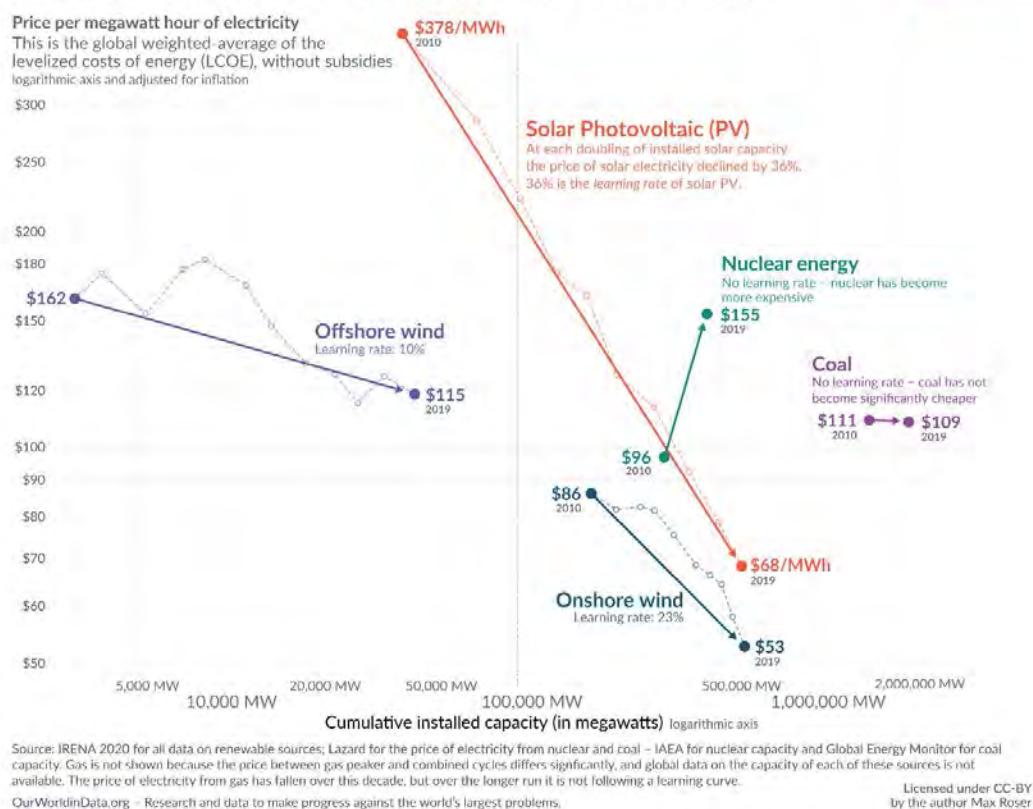


Figure 4: The trend of the LCOE of renewable systems since 2010 to 2019.

2.2 Photovoltaic Systems

In this work, we focus on the design of PV systems. Therefore, we will review the technical characteristics, applications and methods in the design of a photovoltaic station. PV systems are composed of two main components: 1) PV panels, and 2) PV inverters or converters.

A PV panel is composed of PV modules, which contain hundreds of solar cells. Solar cells are electronic devices that essentially convert solar energy of sunlight into electrical energy and are composed of the same principles as semiconductors such as diodes and transistors [15]. Conventional PV panels are configured from serial interconnected subgrouping of cells, which include hundreds of PN junctions connected in parallel. When sunlight is present, an electrostatic field is produced at the PN junction of the PV module by the impinging photons that create a potential difference between 0.5 and 0.6 Volts (V) and a current of several amperes (A) [15].

PV panels generate DC power from sunlight, but do not store electricity, so energy can be stored in batteries if required. An array of PV panels voltages may vary within 300 to 1000 V and currents within 5 to 10 A in a PV system installation [15].

According to their technology, there are three main categories of PV modules: monocrystalline, polycrystalline and thin-film-based materials. Both monocrystalline and polycrystalline PV modules are based on crystalline silicon semiconductor. However, the main difference between these two technologies is the type of silicon solar cell they use. Monocrystalline PV modules have solar cells made from a single crystal of silicon, while polycrystalline ones are made from many silicon fragments melted together [21]. In terms of efficiency, monocrystalline PV modules are more efficient than polycrystalline PV modules because monocrystalline PV modules are cut from a single silicon crystal, which allows electricity to pass easily through the module. Nevertheless, the difference in efficiency between both is not so high and polycrystalline modules have lower cost because the manufacturing process is less complex than monocrystalline modules that need more care and control [15] [21].

Thin-film PV modules are characterized by very fine and thin layers that make it flexible. They can have different sizes and not standardized measures as PV modules made of silicon, however, they have a much lower efficiency than the two previous mentioned. Unlike crystalline PV modules that use silicon, thin-film PV modules are made from different materials such as Cadmium telluride, Amorphous silicon and Copper indium gallium selenide [15] [22]. Figure 5 shows a monocrystalline, a polycrystalline and thin-film PV modules [23].

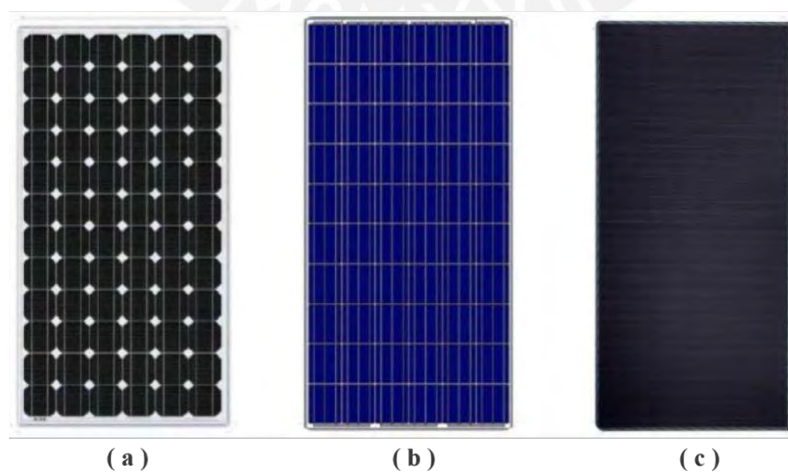


Figure 5: Types of PV modules: (a) Monocrystalline, (b) Polycrystalline, (c) Thin-film.

The other main component in PV systems are the PV inverters. In addition, other complementary components are necessary for the system to work properly, such as: interconnection (i/c) transformer and cable, production and utility meter, and storage battery systems [15] [24]. The transformer is an electrical device responsible for splitting the output voltage of PV inverters and can operate as a step-up or step-down transformer according to the characteristics of the electric grid. As for harmonics, PV inverters typical harmonic content is below 1%, which has almost no impact on the system and with an appropriate regulation of PV inverters, a clear definition of transformer failures can be obtained. [25]. The production meter is a device that measures the amount of energy in kilowatt-hour (kWh) produced by the PV system. A kWh is a measure of how much energy is using per hour. The utility meter is a device that measures the consumption of energy in kWh associated to residential houses, buildings or plants. Storage battery systems store the energy produced by the PV panels and, as explained below, are connected depending on the type of PV inverter systems [15].

This work focuses on the effects of PV inverters for the design of a PV station. As explained above, PV panels generate direct current that can only be used to some devices. However, residential and industrial devices need alternating current. Therefore, PV inverters are components that convert DC power into AC power. In general, PV inverter systems are classified in two categories: stand-alone or grid independent and grid-connected or utility-interactive [15].

Stand-alone PV inverter systems works without a utility grid and are usually connected to battery banks, which provide the DC power. The inverters must be sized to meet the AC demand load requirements, and PV modules are sized to provide adequate charge to support the battery system.

In grid-connected PV systems, inverters are designed to operate in parallel with the electrical utility grid systems. In this, PV modules provide DC power, which is directly connected to the inverters. The AC power produced by the inverters is directly used by the load or, in case of excess power, will synchronously feed the grid system. AC power is directly proportional to the photovoltaic DC source [15]. Alternatively, the PV inverters in a bimodal PV system include specific electronic circuits that allow them to operate in either grid connected or stand-alone mode with a backup system. However, for large PV systems the design with these features is complicated in such as anti-islanding protection, which protects the inverters in case of accidents such as power

outages, and maximum power point tracking (MPPT) [15]. Figure 6, Figure 7 and Figure 8 show examples of stand-alone and grid-connected PV systems and bimodal respectively [26].

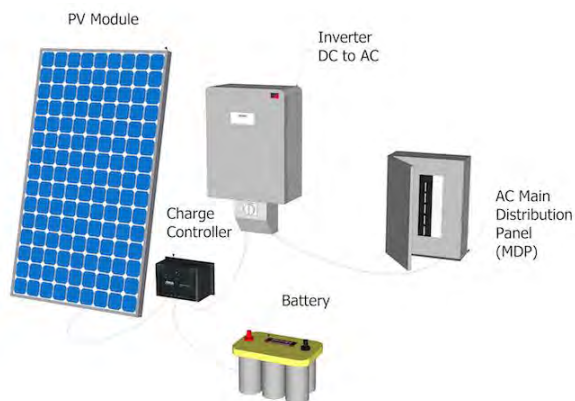


Figure 6: Stand-alone PV system.



Figure 7: Grid-connected PV system.



Figure 8: Bimodal PV system.

PV systems can be classified into three groups according to the type of project or application: Residential, commercial and utility-scale PV systems. Residential PV systems are the smallest of the three projects and, in terms of size, usually consist of 15 to 20 PV modules ranging from 1 to 10 kW [27]. They are typically installed on the roofs of houses. Figure 9 shows an installation of a residential PV system [27]. Commercial PV systems are considered large PV systems and are generally installed on the ground or, occasionally, on the surface of the water (lakes or sea). In terms of size, commercial PV systems consist of an average of 400 PV modules from 10 kW installed size upwards [27]. The definition of a utility-scale PV system is typically determined by size. According to the Solar Energy Industries Association [28], a utility scale project is if the system capacity is from 1 MW upwards; however, for National Renewable Energy Laboratory [29] it is if the system capacity is over 5 MW. Although their definitions may vary, the main objective remains the same: to connect to the grid and sell the generated electricity to the local utility [30] [31]. Figure 10 and show a commercial and Utility-scale PV system [32] [33].



Figure 9: Residential PV system.



Figure 10: Commercial PV system.



Figure 11: Utility-scale PV system.

In this thesis, we will focus on the design of a PV station and consider the following features: A large PV grid-connected station (PVGCS) up to 100 kW, polycrystalline based PV modules, in-depth analysis of PV inverters and their interconnections as the main component of the PV station and, the effects of PV inverter types in terms of investment cost, efficiency and reliability in power generation and power loss. Therefore, the characteristics, methods and operational constraints for the optimal design of PV stations are presented.

2.3 Modelling of a Photovoltaic Station

In [34] and [24], methods to determine the optimal characteristics such as the number of PV panels and PV inverters of the PVGCS are presented. For this purpose, Figure 12 shows the block diagram of a generalized PV station [24]. Several PV inverters are used to interconnect the DC output voltage of the PV modules with the AC requirements of the power grid. The total number of PV modules is determined by the size, characteristics and total number of PV inverters (n_i) and n_i is defined by the maximum capacity allowed by the PV station. An array of PV panels, which we call a PV set, consists of the number of PV panels connected in parallel (n_p), where each PV panel is composed of a number of PV modules connected in series (n_s). A PV set is connected to the DC input of each DC/AC PV inverter.

PV inverters typically have an integrated MPPT system in order to extract the maximum available power from the PV power sources [34]. In addition, PV inverters have surge protection devices (SPD) that protects PV system against direct lightning strokes limiting transient overvoltage

and diverting current waves to earth. The AC output power generated is injected into the electric grid at the point of common coupling (PCC) through an i/c transformer and cable, respectively [24].

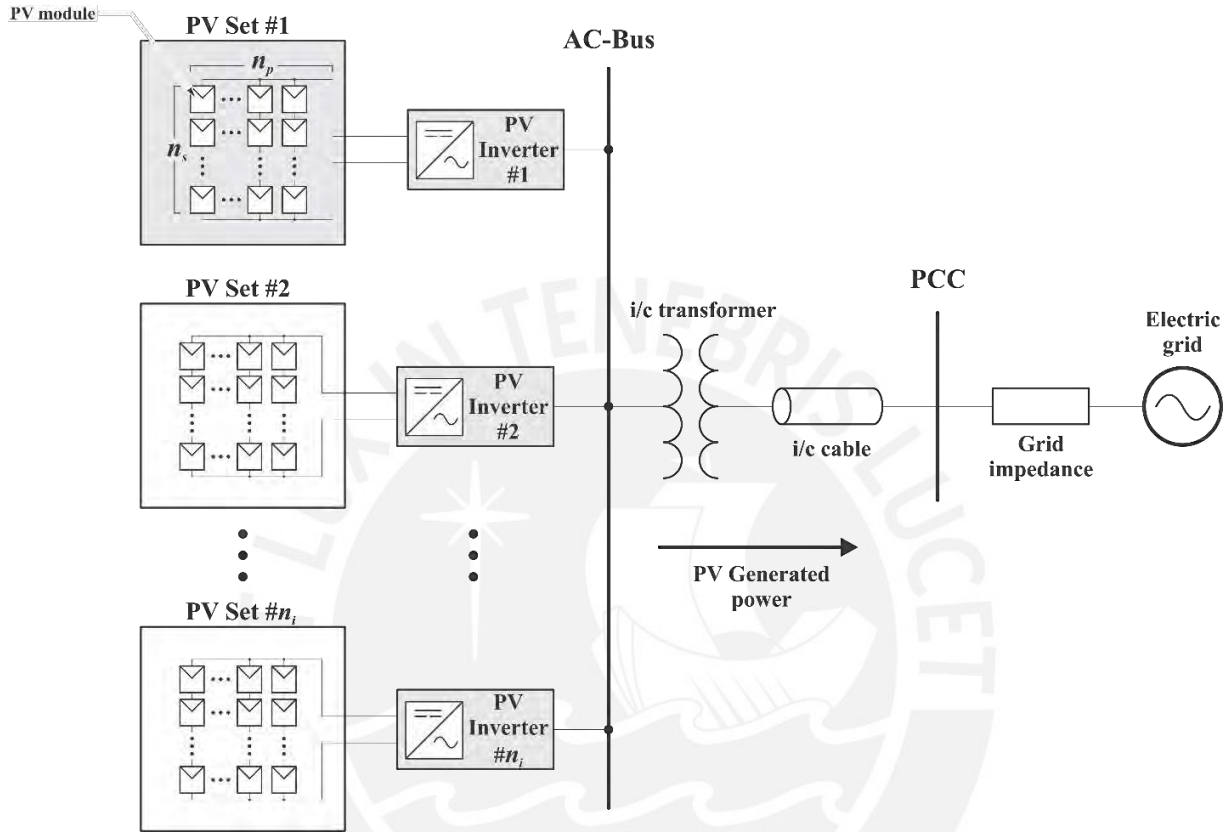


Figure 12: Block diagram of a generalized PV station.

2.4 Optimal Design Methods for Photovoltaic Stations

The effects of tilt and orientation of the PV set on the PV station is investigated in [35]. Figure 13 shows the arrangement of a PV set, where N_r is the number of rows or PV panels n_s of a PV set, L_{pv1} and L_{pv2} are the length and width of each PV module, respectively [34]. β ($^\circ$) is the PV modules tilt angle ($0^\circ \leq \beta \leq 90^\circ$), W_1 and H_1 are the width of the area and the maximum height of a PV module tilted at an angle equal to β° , respectively. Finally, W_T and H_T are the width of the area occupied and the maximum height of each PV set, respectively.

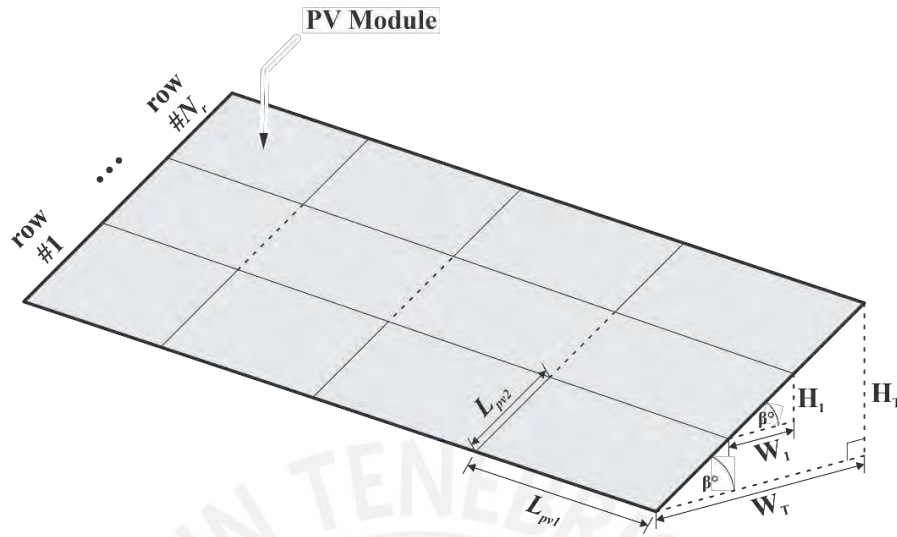


Figure 13: Arrangement of PV set.

Using the technical data of commercial PV modules and considering worldwide estimations of the optimal tilt angles of PV panels in [36], the parameters in the PV set can be calculated and are given by [34]

$$W_1 = L_{pv2} \cos \beta \quad (1)$$

$$W_T = W_1 N_r \quad (2)$$

, and

$$H_1 = L_{pv2} \sin \beta \quad (3)$$

$$H_T = H_1 N_r \quad (4)$$

Figure 14 and Figure 15 show the arrangement of PV sets in blocks and the arrangement and orientation of PV sets in the available installation area, respectively [24] [34]. The adjacent PV sets are installed with an adequate distance between them in order to avoid the mutual shading of the PV panels. The distance required between adjacent blocks F_y is determined as a design variable of the PV station [34]. Taking as a reference in [36] [24], the PV sets are considered to be oriented towards the southern side of the available installation area. However, this may change depending on the available installation location in the design of a PV station. The length of the southern side of the actual installation area D_1 is constrained to be less than the southern dimension of the total available installation area DIM_1 ($D_1 \leq DIM_1$). Similarly, the western

dimension of the actual installation area D_2 is less than the western dimension of the total available installation area DIM_2 ($D_2 \leq DIM_2$).

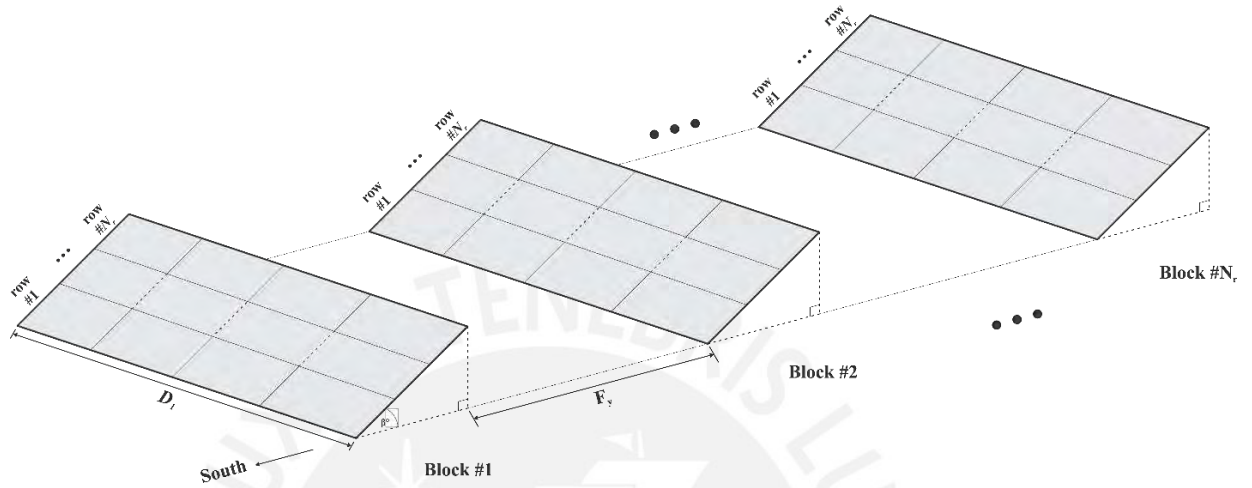


Figure 14: Arrangement of PV sets in blocks.

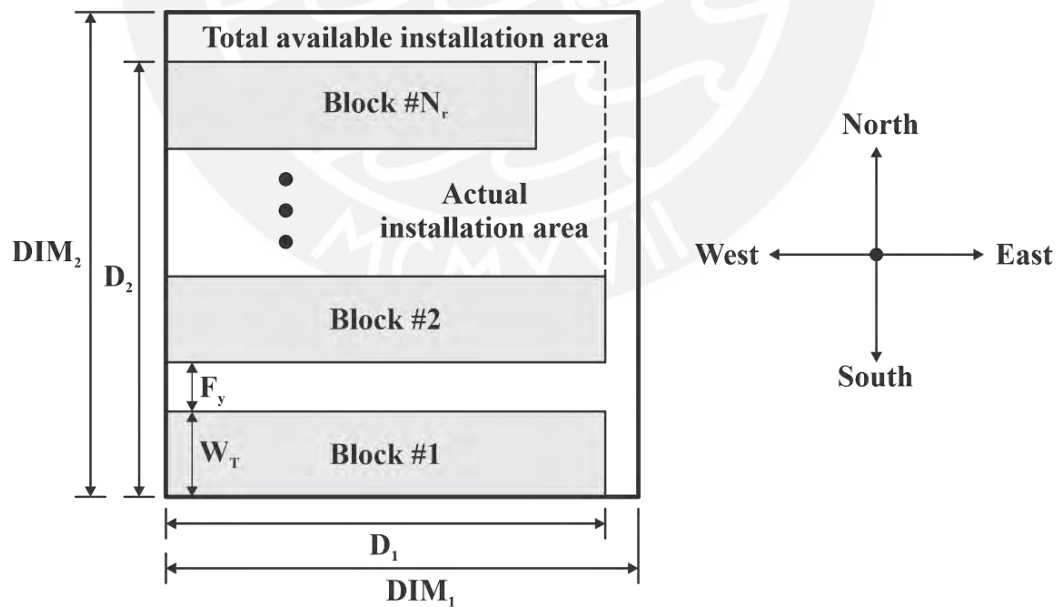


Figure 15: Arrangement and orientation of PV sets in the available installation area.

In [2], an economical design for utility-scale PV stations with optimal availability is presented. First, PV stations are categorized according to their type of topology or structure. Figure 16 shows the basic topologies used in the implementation of PV stations. These topologies represent four structures: Centralized, string, multistring and AC modular [2].

In the centralized topology the PV modules are connected in series to form a branch with a specific voltage level. Then, the series branches are connected in parallel to generate the rated power of the PV station and the generated power is injected to the grid using a single high-power DC/AC PV inverter. The first stage of the PV inverter DC/DC is used to perform MPPT via adjusting the PV operating voltage as explained above. Centralized topology is cost-effective because it uses a single PV inverter; however, its efficiency and reliability decrease as the rated power of the PV plant increases [2].

The string topology divides the PV system into subsystems with independent strings of PV modules connected in series. Each subsystem has a DC/DC converter for the MPPT followed by a DC/AC inverter connected to the grid. Independent MPPT modules improve the captured power efficiency of the PV station; however, it imposes a high investment cost [2].

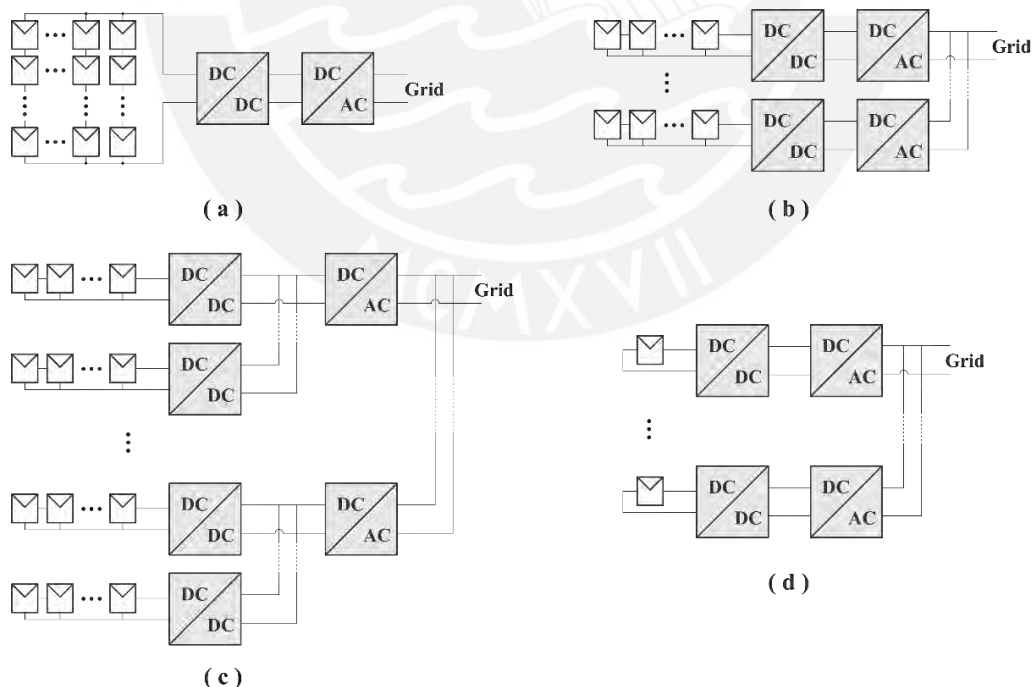


Figure 16: Basic topologies for PV stations: (a) Centralized, (b) string, (c) multistring, and (d) AC modular.

Similar to the string topology, the multistring topology use independent DC/AC grid-connected PV inverters. However, each inverter is linked with more than one PV string with DC/DC converters. This topology is energy efficient because it uses independent MPPT units and it is more cost effective than the string topology [2].

In an AC modular topology, each PV module has a low-power DC/AC PV microinverter, and PV panels are connected via an ac link. Since it uses one MPPT unit per PV module, this topology is very efficient and reliable; however, it is not cost-effective for large PV stations, but can be a great option for small PV projects [2].

The reliability of a PV station requires an estimation of the energy that is not supplied in the PV system and is a function of the total number of PV panels and inverters, the connections and the reliability characteristics of the components. Therefore, two main parameters for reliability assessment are presented. The mean time between failures (MTBF), which is the total operating time divided by the number of failures, and mean time to repair (MTTR), which represents the average repair time of a failed component. Based on these parameters, the failure rate λ and repair rate μ are defined as [2] [37].

$$\lambda = \frac{1}{\text{MTBF}} \quad (5)$$

$$\mu = \frac{1}{\text{MTTR}} \quad (6)$$

The failure and repair rate of the components can be assumed constant values due to the fact that, during the lifetime of the system, components fail randomly through a uniform distribution. Furthermore, the experimental and field studies indicate that, in a PV energy system, the failures dominantly occur in power electronic interfaces. Studies and statistical data show that the reliability of the PV system depends mainly on the number of PV inverters and their interconnection structure. The Markov modelling, which is explained in the next chapter, is presented as a method for determining the failure and repair probabilities of PV components.

In [2], the cost algorithms for the selection of the best energy price option in terms of availability and profitability are presented. The economic design is based on consideration of the current prices of the PV system components and also the current investment and operating costs.

The conventional LCOE, as previously mentioned, is the energy parameter that indicates how much is the cost per energy consumed, in energy theory the unit is, for example, dollar per kilowatt-hour (\$/kWh) and it is defined as [2]

$$\text{LCOE} \triangleq \frac{\text{Total life cycle cost of the plant}}{\text{Generated energy over its physical lifetime}} \quad (7)$$

where, the total cost of the plant includes the initial, maintenance and repair during the life cycle of the power plant. The generated energy is simply the expected generated energy assuming rated power over the physical lifetime of the plant. The detailed calculation of the LCOE is given by [2]

$$\text{LCOE} = \frac{C_i - C_{tr} + C_y - C_{rv}}{E_{tot}} \quad (8)$$

Here, C_i is the initial investment cost, which includes costs of facilities, land, cabling, and planning. C_{tr} is the depreciation tax benefit, C_y is the total annual cost, C_{rv} is the benefit related to the system residual value, and E_{tot} is the total generated energy over the physical lifetime of the PV power plant.

In [3], the trend of LCOE variations for various types of power plants is presented. However, this algorithm to calculate the LCOE is used for centralized topology plants with minimum installation cost. Likewise, it can be used as a cost comparison tool with plants of different topology and configuration. Therefore, a modification of LCOE is introduced in the design of a PV station with optimal availability. This is the effective levelized cost of energy (ELCOE) and in general is given by

$$\text{ELCOE} = \frac{\text{Total effective cost}}{\text{Total effective generated energy}} \quad (9)$$

where, the total effective cost considers not only the costs mentioned above, but also the estimated cost of maintenance and repair or replacement of the PV inverters during the lifetime of the PV plant, using the probabilities and state transitions of the Markov model [2]. The total effective energy generated considers the previous estimation as well.

A cost function of PV inverters in the range from 0.7 up to 250 kW is presented, in order to determine the optimal size of PV inverters for PV power plants in the range of 0.1 to 100 MW is also presented. The results of these methods are based on assuming, for the case study, parameters such as, for example, the time per day that the PV panels generate energy, which in many cases, directly affect the ELCOE values.

2.5 Operational Constraints

In the design, certain technical and operational constraints of the PV station components must be considered. From this, calculations can be performed to demonstrate the proposed algorithms. The technical and operational characteristics of the PV modules and inverters are listed below.

For the optimal design method calculations, we use PV modules from Eco Green Energy Company [38]. Model: EOS POLY 330W-350W 72 Cells.

ELECTRICAL DATA AT STC*

Power output (Pmax)	330 W	335 W	340 W	345 W	350 W
Power tolerance	0~+5 W	0~+5 W	0~+5 W	0~+5 W	0~+5 W
Module efficiency	17.01%	17.27%	17.52%	17.78%	18.04%
Module efficiency	37.93 V	38.15 V	38.42 V	38.68 V	38.93 V
Maximum power current (Imp)	8.70 A	8.78 A	8.85 A	8.92 A	8.99 A
Open circuit voltage (Voc)	46.11 V	46.32 V	46.58 V	46.85 V	47.12 V
Short circuit current (Isc)	9.10 A	9.16 A	9.23 A	9.31 A	9.38 A

*Standard Test Conditions: Irradiance: 1 000 W / m² • Cell temperature: 25°C • AM: 1.5

Table 1: PV module electrical data at Standard Test Conditions.

ELECTRICAL DATA AT NMOT*

Power output (Pmax)	244.13 W	247.83 W	251.53 W	255.23 W	258.92 W
Maximum power voltage (Vmp)	35.03 V	35.23 V	35.48 V	35.72 V	35.96 V
Maximum power current (Imp)	6.96 A	7.02 A	7.08 A	7.14 A	7.19 A
Open circuit voltage (Voc)	42.80 V	43.00 V	43.24 V	43.49 V	43.74 V
Short circuit current (Isc)	7.39 A	7.44 A	7.49 A	7.56 A	7.61 A

*Nominal Operating Cell Temperature: Irradiance: 800 W / m² • Ambient temperature: 20°C
• AM: 1.5 • Wind speed: 1 m/s

Table 2: PV module electrical data at Nominal Operating Cell Temperature.

MECHANICAL CHARACTERISTICS

Cell type	Polycrystalline (156.75x156.75mm)
Number of cells	72
Dimensions	1956x992x40mm
Weight	22.8 kg
Glass	3.2 mm tempered glass, High transmission (>94%), Anti-Reflective Coating
Frame	Anodized aluminium alloy
Junction box	IP68 rated (3 by pass diodes)
Cable	4mm ² , 900mm (+) 900mm (-); Length can be customized
Connector	MC4 or MC4 compatible
Max front load (e.g.: snow)	5400 Pa
Max back load (e.g.: wind)	2400 Pa

Table 3: PV module mechanical characteristics.

For PV inverters, Huawei brand inverters are considered. In this work, the following PV inverter models are considered: SUN2000-12-20KTL-M2 [39], SUN2000-30-40KTL-M3 [40], SUN2000-(50KTL, 60KTL, 65KTL)-M0 [41] and SUN2000-100KTL-M1 [42].

The characteristics of a PV inverter model SUN2000-100KTL-M1 are described:

TECHNICAL SPECIFICATION: SUN2000-100KTL-M1 [42]

EFFICIENCY:

Max. efficiency	98.8% @480 V, 98.6% @380 V / 400 V
European efficiency	98.6% @480 V, 98.4% @380 V / 400 V

Table 4: Huawei 100 kW PV inverter efficiency specifications.

INPUT:

Max. Input Voltage	1,100 V
Max. Current per MPPT	26 A
Max. Short Circuit Current per MPPT	40 A
Start Voltage	200 V
MPPT Operating Voltage Range	200 V ~ 1,000 V
Nominal Input Voltage	720 V @480 Vac, 600 V @400 Vac, 570 V @380 Vac
Number of MPP trackers	10
Max. input number per MPP tracker	2

Table 5: Huawei 100 kW PV inverter input specifications.

OUTPUT:

Nominal AC Active Power	100,000 W
Max. AC Apparent Power	110,000VA
Max. AC Active Power (cosφ=1)	110,000 W
Nominal Output Voltage	480 V/ 400 V/ 380 V, 3W+(N)+PE
Rated AC Grid Frequency	50 Hz / 60 Hz
Nominal Output Current	120.3 A @480 V, 144.4 A @400 V, 152.0 A @380 V
Max. Output Current	133.7 A @480 V, 160.4 A @400 V, 168.8 A @380 V
Adjustable Power Factor Range	0.8 leading... 0.8 lagging
Max. Total Harmonic Distortion	<3%

Table 6: Huawei 100 kW PV inverter output specifications.

GENERAL DATA:

Dimensions (W x H x D)	1,035 x 700 x 365 mm
Weight (with mounting plate)	90 kg
Operating Temperature Range	-25°C ~ 60°C
Cooling Method	Smart Air Cooling
Max. Operating Altitude without Derating	4,000 m
Relative Humidity	0 ~ 100%
DC Connector	StaubliMC4
AC Connector	Waterproof Connector + OT/DT Terminal
Protection Degree	IP66
Topology	Transformerless
Nighttime Power Consumption	< 3.5 W

Table 7: Huawei 100 kW PV inverter general data.

In this case, the Huawei 100 kW PV inverter features 10 MPP trackers, where each MPP tracker supports up to two signal inputs, in order to get the maximum power from the PV station. Figure 17 shows the circuit diagram of Huawei 100 kW PV inverter interconnection, where it can be seen that SPD protection against return current from lightning strikes is embedded in both the input and output of the PV inverter. Figure 18 represents a Huawei 100 kW PV inverter [42].

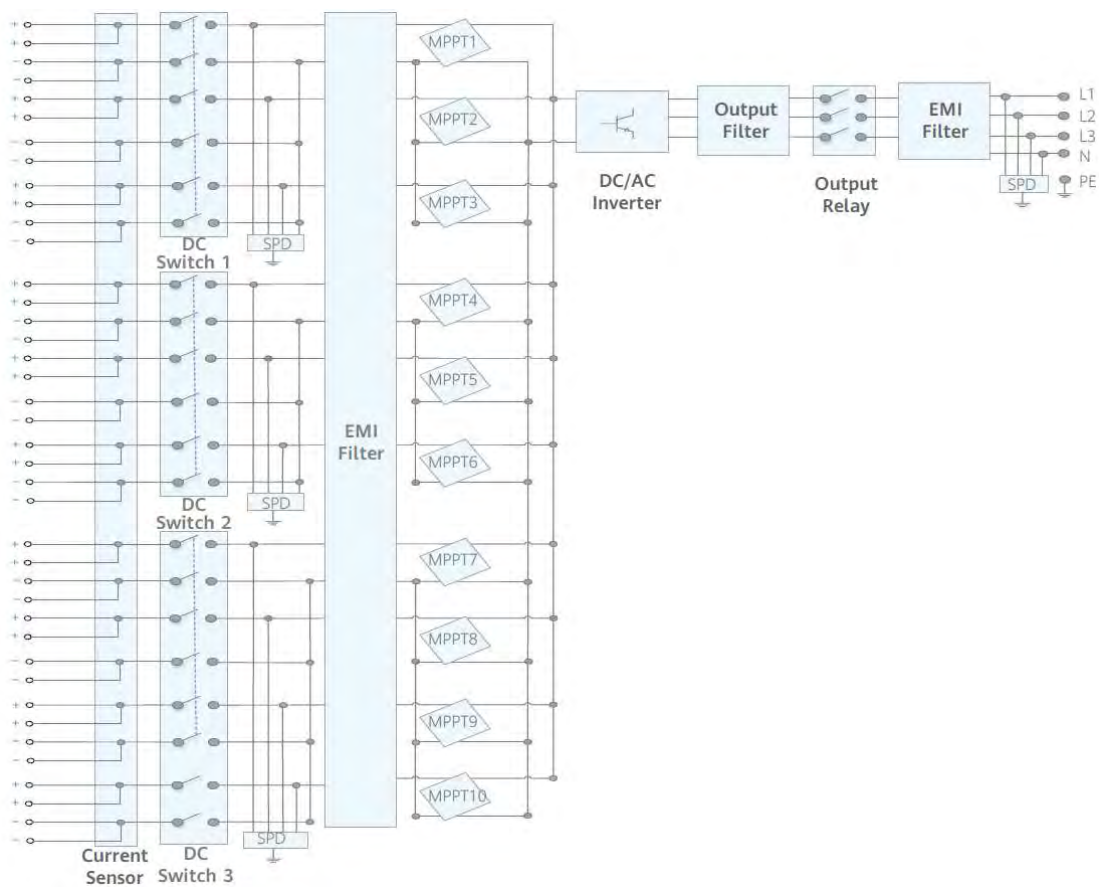


Figure 17: Circuit diagram of Huawei 100 kW PV inverter interconnection.



Figure 18: Huawei 100 kW PV inverter.

Chapter 3: Optimal Design Method

3.1 Markov Modelling

The Markov modelling is a technique that can be applied to systems with random behavior that vary discretely or continuously with respect to time and space [37]. This discrete or continuous variation is known as a stochastic model. A stochastic process [43] has non-deterministic behavior and the subsequent states are determined by predictions and by random elements. Solar powered systems are characterized by a stochastic behavior due to the intermittent solar radiation, and therefore, there is a huge challenge to develop smart algorithms, methods and tools to quantify their reliability [5].

The Markov model, also called Markov chains, consists of a sequence of possible events where each future transition depends only on the current state and not on previous states. In addition, the process must be stationary or homogeneous for the Markov approach to be applicable, that means that behavior of the system must be the same at all points of time. In the case of system reliability evaluation, the space is represented as discrete functions and is composed of discrete and identifiable states [37].

Figure 19 represents a two-state example A and B of the Markov chain, where each number on the arrow represents the probability of changing from one state to another state [37]. Consider the first-time interval and assume the system is initially in state A. The probability of changing state to B is 0.8, while the probability of remaining in the same state is 0.2. The sum of these probabilities, remaining in or moving out of a state, must be unity. Similarly, if the current state is B, the probability of changing to state A and remaining in the same state is 0.3 and 0.7, respectively.

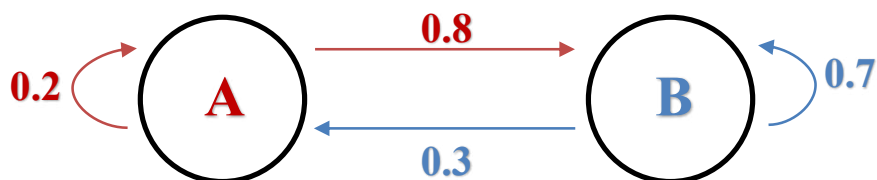


Figure 19: Example of two-state Markov chain.

Figure 20 represents the behavior of the system using the tree diagram [37]. This figure assumes that the system starts at state A, shows the states after each time interval or step and considers up to 4 such time intervals. The probability of continuing on any branch of this tree can be assessed by multiplying the appropriate probabilities of each step of this branch. The probability of being in a certain state of the system after a certain number of time intervals is then evaluated by summing the probabilities of the branches leading to that state after the number of time intervals considered. If these branch probabilities leading to state 1 are summed, the probability of residing in state 1 after 4-time intervals is $43/128$, while a similar sum would show that the equivalent probability of residing in state 2 is $85/128$ [37] [44].

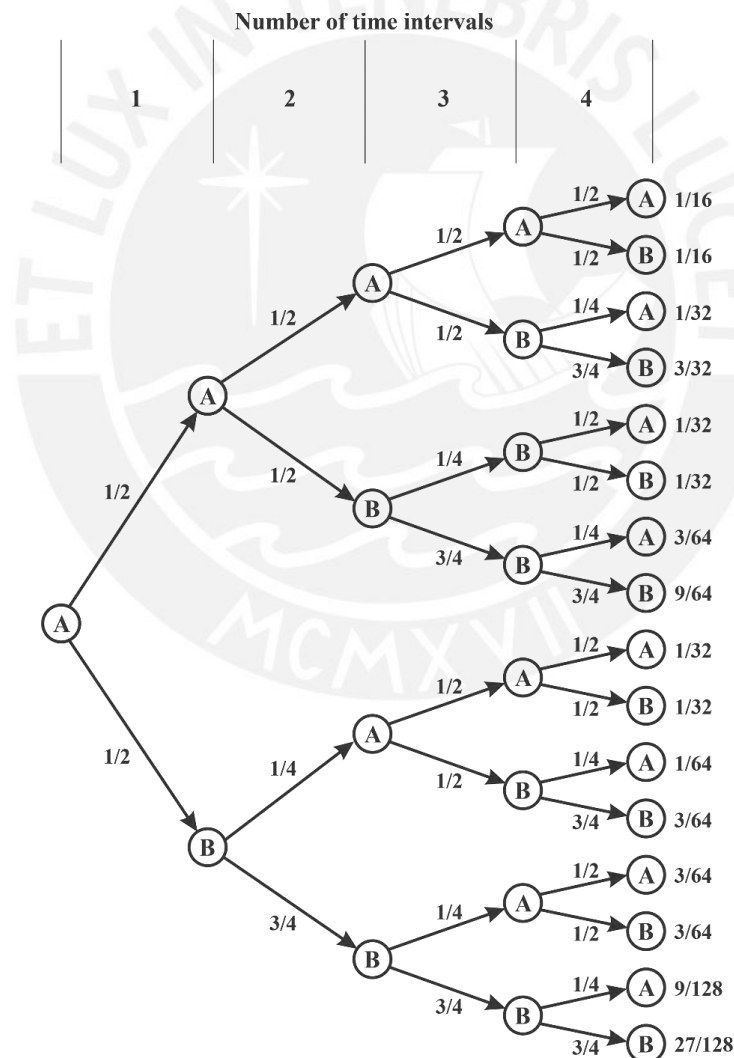


Figure 20: Tree diagram of two-state system.

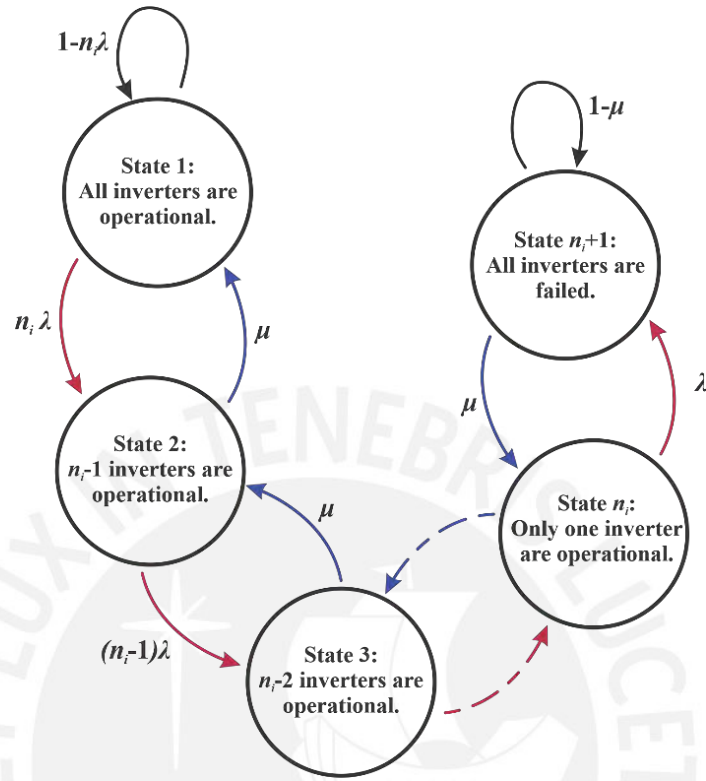


Figure 21: Markov model states and transitions of a PV system.

For our case, in the Markov model in a PV System, the total number of states is $n_i + 1$, where n_i is the number of PV inverters of a PV Station. Figure 21 shows Markov model states and transitions of a PV system with n_i inverters [2].

Figure 22 represents a two-state ($n_i = 1$) system transient behavior or time-dependent values of the state probabilities. As the number of time intervals (NTIs) on the x-axis increases, the y-axis probability state values tend to be constant and is characteristic of systems satisfying the conditions of the Markov model. This steady state is called the limit state or time-independent of the state probabilities. In this example, the system is assumed to start in the state 1 (as in Figure 21, all inverters are operational) and its behavior is evaluated as time increases. The state 2 or at zero time (all inverters are failed) is known as the initial conditions and in most reliability evaluations these conditions are known [37]. Similarly, Figure 23 shows a five-state ($n_i = 4$) system transient behavior, where the sum of the probabilities in the steady state is one.

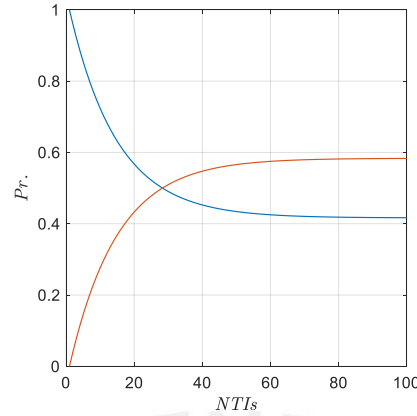


Figure 22: two-state system transient behavior.

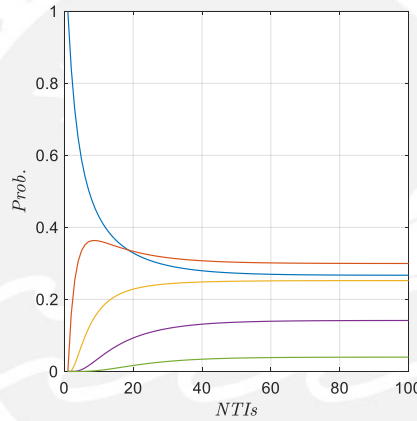


Figure 23: Five-state system transient behavior.

The Stochastic transitional probability matrix (STPM) is used to evaluate reliability. To do this, it is necessary to obtain a matrix which represents the probabilities of making a transition from one state to another in a time interval [37]. If we consider, as an example, the two-state system in Figure 19, the transitions are represented by the following matrix P

$$P = \begin{bmatrix} P_{11} & P_{12} \\ P_{21} & P_{22} \end{bmatrix} = \begin{bmatrix} 1/2 & 1/2 \\ 1/4 & 3/4 \end{bmatrix} \quad (10)$$

where, P_{ij} is the probability of making the transition to state j after a time interval given, that it was in state i at the beginning of the time interval [37].

3.2 Energy Price Modelling

This section introduces a price model based on [2]. In [2], the following formula was used to estimate the cost of a PV inverter as

$$C_1(x) = \alpha_1 + \alpha_2 x - \alpha_3 x^2 + \alpha_4 x^3 \quad (11)$$

where x is the size of the inverter in kW and $C(x)$ is in U.S. dollars (USD) (\$) and $\alpha_1 = 660$, $\alpha_2 = 480$, $\alpha_3 = 0.55$, $\alpha_4 = 0.0005$. For practical calculation purposes, this work does not consider price changes or adjustments for inflation over time.

In this work, the current price trend for commercial PV inverters [45] [46] [47] and the formula presented in [2] are used to develop a new price model to the PV inverters up to $x_{\max} = 100$ kW. Figure 24 shows the flow diagram of this model. According to the above equation, the price per 1 kW of PV inverter in 2012 is equal to \$1140.

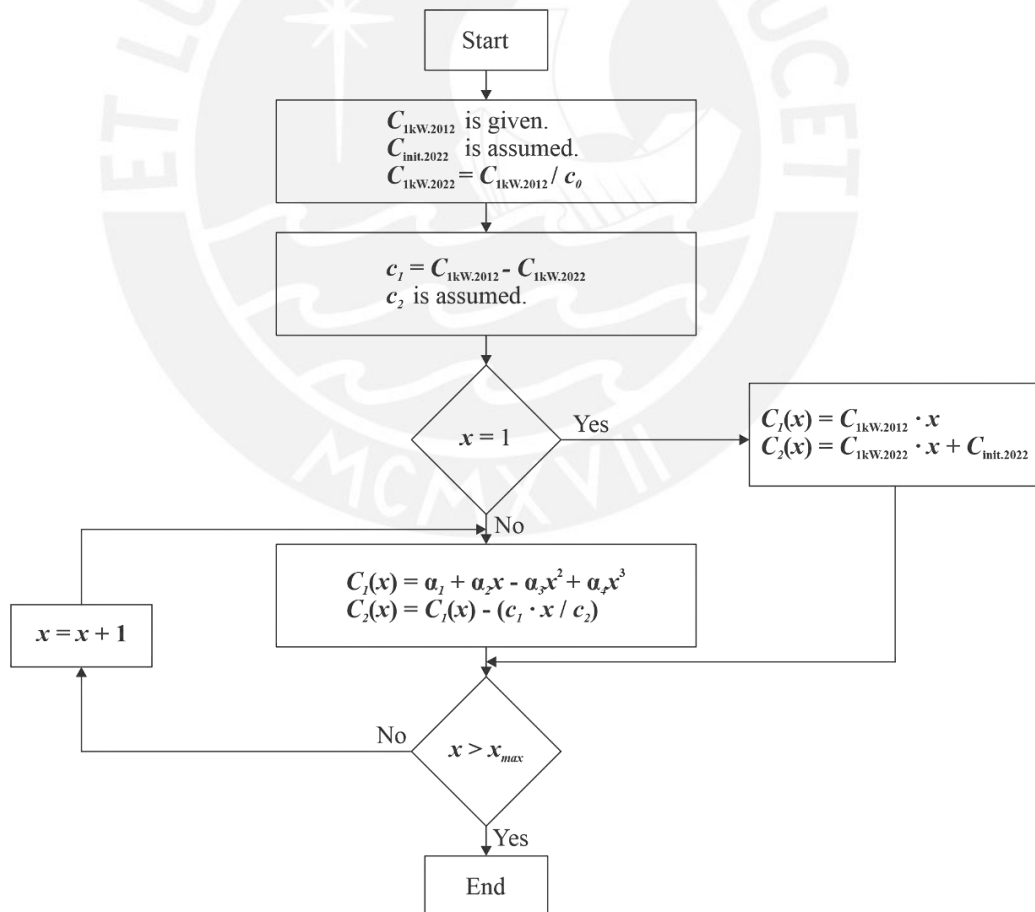


Figure 24: New energy price model flow diagram.

Based on commercial data, we consider the price per kW of PV inverters in 2022 to be 4 times lower than 10 years ago. In contrast to the model in [2], in this new model we consider two calculation factors. The first factor c_1 is the difference between current and 2012 prices per kW. The second factor c_2 is assumed to be equal to 3 to simulate the fall in component prices and the increase in efficiency [47]. We consider an initial price factor of 1kW PV inverter equal to \$600 in the cost estimation when $x = 1$, that is, in the centralized topology. Therefore, the new energy price model in 2022 $C_2(x)$ is given by

$$C_2(x) = C_1(x) - \left(\frac{c_1 \cdot x}{c_2} \right) \quad (12)$$

In addition, an initial cost factor of the inverters at the current time is considered.

Figure 25 shows the trend of the cost of inverters with respect to their size, where the price has changed significantly in 10 years according to the current commercial data. In 2022, the cost of 1 kW inverter is lower than in 2012 based on the new pricing model in the proposed method.

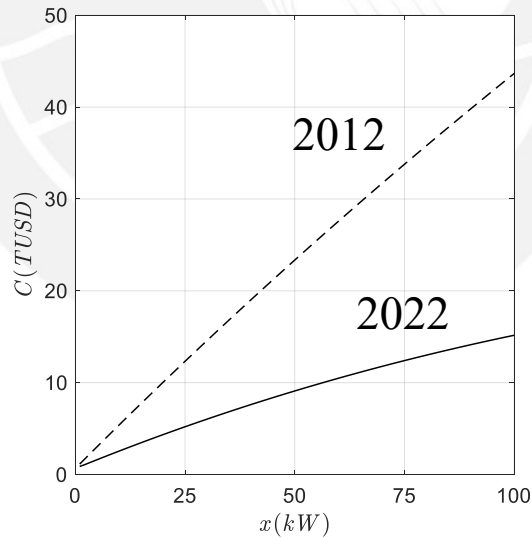


Figure 25: Cost of PV inverters versus inverter size.

3.3 Proposed Optimal Design Method

The following proposed optimal design method is used for the design up to 100 kW large PV station. Figure 26 represents the real data of the injected energy is available from a reference PV station in Langewiesen, Germany and is available from the Department of Automation Engineering, Technical University of Ilmenau.

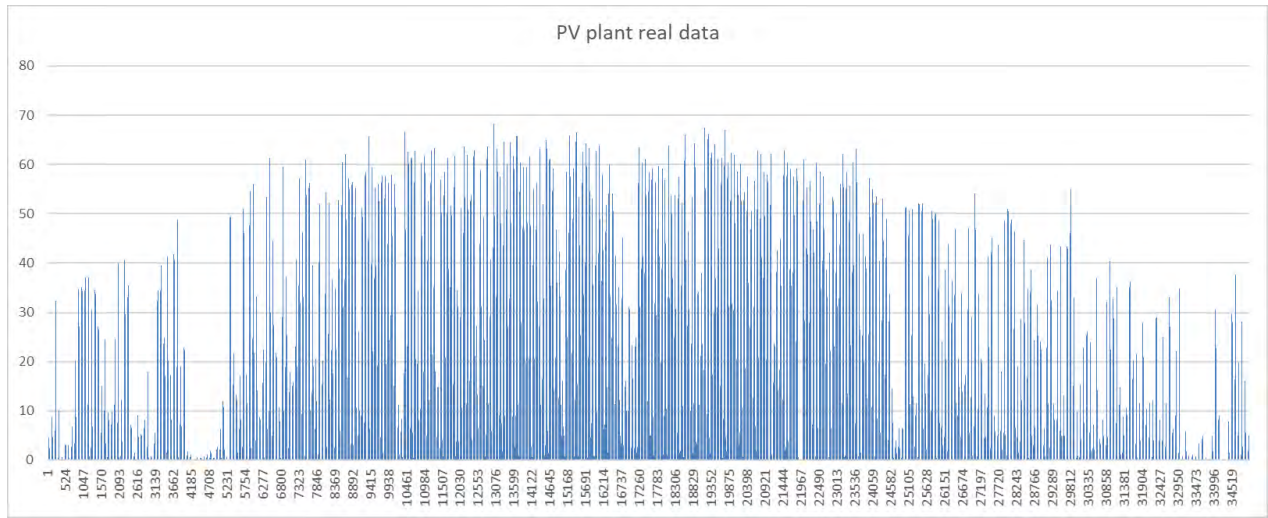


Figure 26: The real data of the injected energy is available from a reference PV station in Langewiesen, Germany.

Important features of the actual data are presented:

- The installed peak power of PV panels P_{tot} is equal to 86 kWp.
- Four samples per hour for one year, that is, 35,040 samples.
- The real sum of the PV modules generated in a year P_{real} is 73,713 kWh
- The ideal sum of the PV modules generated in a year P_{ideal} is 749,295 kWh
- The maximum power generated is 68 kW

The average hours per day that a PV module generates its rated power can be defined as [2]

$$h \triangleq \frac{TGEY}{365 \cdot P_{tot}} \quad (13)$$

where $TGEY$ is the total amount of generated energy in a year in kWh. However, in [2] the value of h is equal to 6 h based on a geographical location. Therefore, in this work we calculated the $TGEY$ based on the available data as

$$TGEY = IGEY \cdot PV_{factor} \quad (14)$$

where $IGEY$ is the ideal amount of generated energy in a year in kWh which is calculated as

$$IGEY = P_{tot} N_D N_H \quad (15)$$

Here, $N_D = 365$ is the number of days per year and $N_H = 24$ is the number of hours per day, while PV_{factor} is defined as

$$PV_{factor} = \frac{P_{real}}{P_{ideal}} \quad (16)$$

Using the real data, we have $PV_{factor} = 0.098 \approx 0.1$. This gives $h = 2.4$ h and it is lower than the value given in [2].

Now, assuming that x is the optimal PV inverter size in kW to be calculated for a power plant with P_{tot} rated power, then the required number of inverters n_i is shown in the following equation

$$n_i(x) = \left\lceil \frac{P_{tot}}{x} \right\rceil \quad (17)$$

where the ceiling function $[z]$ rounds up the value of z to the nearest integer.

The initial cost of PV inverters includes the procurement cost of inverters plus the transportation/installation costs, this is estimated to be 20% of the acquisition cost of the inverters. Then the initial cost described is given by

$$C_{i(inv)} = 1.2n_i(x)C_2(x) \quad (18)$$

Using the commercial technical data of the PV modules and inverters we can calculate the minimum number of modules $n_{s,min}$ that are connected in series in each PV string and is given by [24]

$$n_{s,min} = \min \left[\text{floor} \left(\frac{V_{i,max}}{V_{PV}} \right), \text{floor} \left(\frac{V_{DC,max}}{V_{oc,max}} \right) \right] \quad (19)$$

where, $V_{i.\max}$, V_{PV} , $V_{DC.\max}$ and $V_{oc.\max}$ are the PV inverter DC input maximum MPP voltage, the rated voltage of PV panels in a PV power plant, PV inverter maximum permissible DC input voltage and PV module maximum open-circuit voltage, respectively.

The number of inverters connected in series and in parallel is considered in the following equations,

$$n_s = \text{ceil} \left[\frac{V_x}{V_{PV}} \right] \quad (20)$$

$$n_p = \text{floor} \left[\frac{\frac{P_{tot}}{n_i}}{\frac{n_{s.\min}}{P_{PV}}} \right] \quad (21)$$

where, V_x and P_{PV} are the DC-side voltage of the PV inverter and the rated power of a PV module, respectively. For the calculation of the number of PV modules in parallel, the *floor* function $[z]$ is considered where this rounds down the value of z to the nearest integer. The latter is in order to avoid problems with the limit values indicated in the data sheet of the PV system components.

The maximum power that each PV inverter can receive is given by,

$$P_{\max}(x) = V_{\max}(x)I_{\max}(x)k_e \quad (22)$$

where, P_{\max} , V_{\max} , I_{\max} are the maximum power, voltage and current of a PV set, respectively, and k_e is the efficiency factor due to the losses of the PV modules and the system connections.

Based on [2], the failure rate λ and repair rate μ are calculated to determine the effect of the inverter size on the operation of the PV plant. The failure rate is based on the failure rate of the high-power electronic switches and in the case of a PV system, the switches are the most sensitive components of the inverter. The standard form of λ for power electronic switches [48] is given by,

$$\lambda = \lambda_b \cdot \pi_A \cdot \pi_E \cdot \pi_Q \cdot \pi_T \left[\frac{\text{Failures}}{10^6 \text{ hours}} \right] \quad (23)$$

where, λ_b , π_A , π_E , π_Q and π_T are the base failure rate, application factor, the operation environment factor, the quality factor and the temperature factor, respectively. Converting the time of each failure to years we get that $10^6 \text{ hours} = 114 \text{ years}$. Using the information in [48] and [49], the base failure rate λ_b is usually expressed by a model, relating the influence of electrical and temperature stresses on the device. Therefore, $\lambda_b = 0.012$ failures per 114 years for a transistor type switch. For PV inverter size $x \geq 250$ W and based on the rating of the switch, $\pi_A = 10$. The environmental factor $\pi_E = 1$ for PV inverters which are often installed on the ground. The quality factor implies the effect of device packaging and considering the worst scenario, that means a transistor with plastic package, $\pi_Q = 8$. The temperature factor is related with the effect of the transistor junction temperature T_j on the failure rate and is calculated by,

$$\pi_T = \exp\left(-1925\left(\frac{1}{T_j + 273} - \frac{1}{298}\right)\right) \quad (24)$$

and T_j is given by,

$$T_j = T_a + P_{loss} R_{\theta_{ja}} \quad (25)$$

where T_a , P_{loss} and $R_{\theta_{ja}}$ is the maximum ambient temperature in °C, the inverter power loss and the thermal resistance between the junction and ambient, respectively. Based on information in [2], [48] and [50], $T_a = 55^\circ\text{C}$, $R_{\theta_{ja}} = 52.6^\circ\text{C/W}$ and $P_{loss} = (1-\eta)x$, where η is the efficiency of the PV power system and it is calculated by $\eta = \eta_c \eta_i$, where η_c is the efficiency of cabling which is about 98% and η_i the efficiency of the inverters and its interconnection with PV panels which is about 97%.

According to the above data we have the following equation,

$$\lambda(Ta) = \lambda_b \cdot \pi_A \cdot \pi_E \cdot \pi_Q \left[\frac{\text{Failures}}{114 \text{ years}} \right] \quad (26)$$

where $\lambda(Ta)$ is calculated with the above values in the worst-case scenario in order to obtain the optimum failure factor. Then replacing in the main equation to determine λ_b , we obtain,

$$\lambda = \frac{\lambda(Ta) \cdot \pi_T \left[\frac{Failures}{1-year} \right]}{114} \quad (27)$$

To determine the repair rate, the estimated days for repair or maintenance the inverters are classified into five groups according to the size of the PV inverter [2]. Table 8 shows the inverter repair time data.

Inverter Size (kW)	$T_d = \text{MTTR}$ (days)
$x \leq 20$	1
$20 < x \leq 50$	7
$50 < x \leq 75$	21
$75 < x \leq 100$	35
$x > 100$	40

Table 8: PV inverter repair time data.

T_d is the same as MTTR and represents the time in days it takes to repair the PV inverter. In the case of the small-size inverters up to 20 kW we assume that these components are easy to repair or replace as plug and play, therefore such repairs can be done by technicians in less than a day. For larger inverters above 100 kW, these are installed as high-power stations. Therefore, the time to repair each inverter is longer and requires qualified specialists and engineers. According to the data shown in the Table 8 the repair rate of PV inverters is given by,

$$\mu = \frac{1}{T_d} \left[\frac{Repair}{1-year} \right] \quad (28)$$

Using the Markov model described above, the stochastic transitional probability matrix A is calculated and shown below [2],

$$A = \begin{bmatrix} 1-n_i\lambda & n_i\lambda & 0 & 0 & \dots & 0 \\ \mu & 1-\mu-(n_i-1)\lambda & (n_i-1)\lambda & 0 & \dots & 0 \\ 0 & \mu & 1-\mu-(n_i-2)\lambda & (n_i-2)\lambda & \dots & 0 \\ 0 & 0 & \mu & 1-\mu-(n_i-3)\lambda & \dots & \vdots \\ \vdots & \vdots & \vdots & \vdots & \vdots & \lambda \\ 0 & 0 & 0 & 0 & \mu & 1-\mu \end{bmatrix} \quad (29)$$

Where for example, the off-diagonal entity a_{ij} is equal to the transition from the state i to state j . The entities on the diagonal a_{ii} is equal to $1-b_i$, where b_i is the sum of the exit transitions of state i . The first element $a_{11} = 1 - n_1\lambda$ and the last element $a_{n_{i+1}n_{i+1}} = 1 - \mu$ of the matrix represents, respectively, the transition to the same state.

Furthermore, the operating probabilities of the PV system are determined to estimate the system availability. A method for calculating these probabilities is presented in [2] and [4]. Based on this method, if p_k is the probability of being in state k , then the state probability vector P is obtained as

$$P = PA \quad (30)$$

where

$$P = [p_1 \quad p_2 \quad p_3 \quad p_4 \quad \dots \quad p_{n_i} \quad p_{n_i+1}] \quad (31)$$

The values obtained for different numbers of PV inverters are shown below. They are observed so that the Markov model rule is satisfied, where the sum of the values in each row is equal to unity.

$$A|_{n_i=1} = \begin{bmatrix} 0.8362 & 0.1638 \\ 0.0286 & 0.9714 \end{bmatrix} \quad (32)$$

$$A|_{n_i=2} = \begin{bmatrix} 0.8394 & 0.1606 & 0 \\ 0.1429 & 0.7768 & 0.0803 \\ 0 & 0.1429 & 0.8571 \end{bmatrix} \quad (33)$$

$$A|_{n_i=3} = \begin{bmatrix} 0.8593 & 0.1407 & 0 & 0 \\ 0.1429 & 0.7633 & 0.0938 & 0 \\ 0 & 0.1429 & 0.8102 & 0.0469 \\ 0 & 0 & 0.1429 & 0.8571 \end{bmatrix} \quad (34)$$

$$A|_{n_i=4} = \begin{bmatrix} 0.8396 & 0.1604 & 0 & 0 & 0 \\ 0.1429 & 0.7368 & 0.1203 & 0 & 0 \\ 0 & 0.1429 & 0.7769 & 0.0802 & 0 \\ 0 & 0 & 0.1429 & 0.8170 & 0.0401 \\ 0 & 0 & 0 & 0.1429 & 0.8571 \end{bmatrix} \quad (35)$$

$$A|_{n_i=5} = \begin{bmatrix} 0.8305 & 0.1695 & 0 & 0 & 0 & 0 \\ 0.5000 & 0.3644 & 0.1356 & 0 & 0 & 0 \\ 0 & 0.5000 & 0.3983 & 0.1017 & 0 & 0 \\ 0 & 0 & 0.5000 & 0.4322 & 0.0678 & 0 \\ 0 & 0 & 0 & 0.5000 & 0.4661 & 0.0339 \\ 0 & 0 & 0 & 0 & 0.5000 & 0.5000 \end{bmatrix} \quad (36)$$

$$A|_{n_i=6} = \begin{bmatrix} 0.8302 & 0.1698 & 0 & 0 & 0 & 0 & 0 \\ 0.5000 & 0.3585 & 0.1415 & 0 & 0 & 0 & 0 \\ 0 & 0.5000 & 0.3868 & 0.1132 & 0 & 0 & 0 \\ 0 & 0 & 0.5000 & 0.4151 & 0.0849 & 0 & 0 \\ 0 & 0 & 0 & 0.5000 & 0.4434 & 0.0566 & 0 \\ 0 & 0 & 0 & 0 & 0.5000 & 0.4717 & 0.0283 \\ 0 & 0 & 0 & 0 & 0 & 0.5000 & 0.5000 \end{bmatrix} \quad (37)$$

An important fact to know for the optimal design is the calculation of the not-supplied expected energy NSEE, which represents the energy that is expected not to be supplied by the system due to component failures or other operational factors. The value of $NSEE_k$ associated with the state k , in which $k-1$ inverters are out of service and is given by [2],

$$NSEE_k = (k-1) \cdot x \cdot h \cdot T_d \quad (38)$$

To calculate the NSEE, the probability of being in state k is assumed to be p_k which is determined from the vector P and is defined by,

$$NSEE = \sum_{k=1}^{n_i+1} p_k NSEE_k = \sum_{k=1}^{n_i+1} p_k (k-1) \cdot x \cdot h \cdot T_d \quad (39)$$

where k ranges from $k=2$ for the centralized topology to $k=n_i+1$ for the other topologies.

The $ELCOE_i$ index as the core of the proposed design algorithm is calculated as follows [2]

$$\text{ELCOE}_i = \frac{C_{t(inv)}}{E_{y(eff)}} \quad (40)$$

where $C_{t(inv)}$ and $E_{y(eff)}$ are total inverter cost during the lifetime of the PV energy system and the amount of effective generated energy in a year, respectively. $C_{t(inv)}$ is defined by

$$C_{t(inv)} = C_{i(inv)} + C_{r(inv)}N \quad (41)$$

where $C_{r(inv)}$ represents the estimation of repair or replacement costs of inverters in a year in USD/year and N is the lifetime of the PV system in years. $C_{r(inv)}$ is determined by

$$C_{r(inv)} = \sum_{k=1}^{n_i+1} p_k \left((k-1)rr + wT_{d_k} \right) \quad (42)$$

where p_k is calculated on the Markov method, $T_{d_k} = (k-1)\text{MTTR}$ represents the downtime of the $(k-1)$ faulty PV inverters, w is the wage for skilled workers during the downtime and rr is the repair cost of the inverters and is given by the following table [2]:

Inverter Size (kW)	Repair Cost (rr) (% of the inverter price)
$x \leq 20$	20
$20 < x \leq 50$	20
$50 < x \leq 75$	18
$75 < x \leq 100$	18
$x > 100$	15

Table 9: Inverter repair cost data.

The amount of effective generated energy in a year of the PV plant is given by the following equation

$$E_{y(eff)} = \sum_{k=1}^{n_i+1} p_k \eta h (n_i + 1 - k) (365 - T_d) x \quad (43)$$

where state probabilities, interconnection efficiency, repair time and PV inverter size are considered.

The flowchart shown in Figure 27 summarizes the proposed optimal design method.

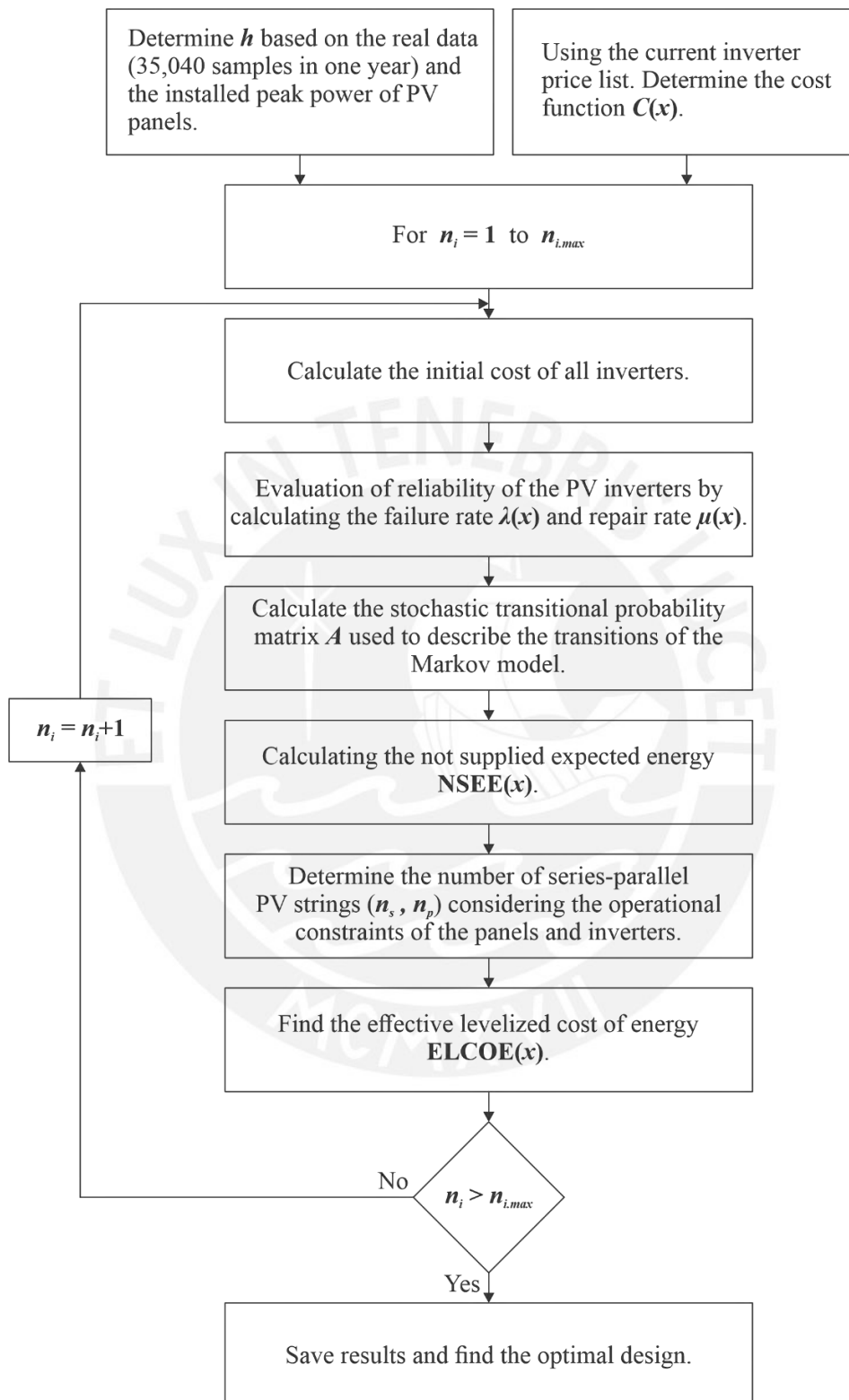


Figure 27: Flowchart for optimal design.

Chapter 4: Results

4.1 System Description

In order to determine the optimal design of a PV station, six cases with six different sizes of real PV inverters were performed which are: $n_i = 1$, $n_i = 2$, $n_i = 3$, $n_i = 4$, $n_i = 5$ and $n_i = 6$; that is, for 100 kW, 50 kW, 30 kW, 25 kW, 20 kW and 15 kW, respectively. The above operating constraints have been considered and for all cases the peak power of the PV station is 86 kWp.

Figure 28 shows the configuration of a PV station with $n_i = 1$ and a PV inverter size equal to 100 kW. The input values of the PV inverter are: $V_{DC,max} = 934.32$ V, $I_{DC,max} = 98.89$ A and $P_{max} = 85$ kWp.

Figure 29 shows the configuration of a PV station with $n_i = 5$ and each PV inverter is of size equal to 20 kW. The input values of each PV inverter are: $V_{DC,max} = 934.32$ V, $I_{DC,max} = 17.98$ A and $P_{max} = 16.46$ kWp.

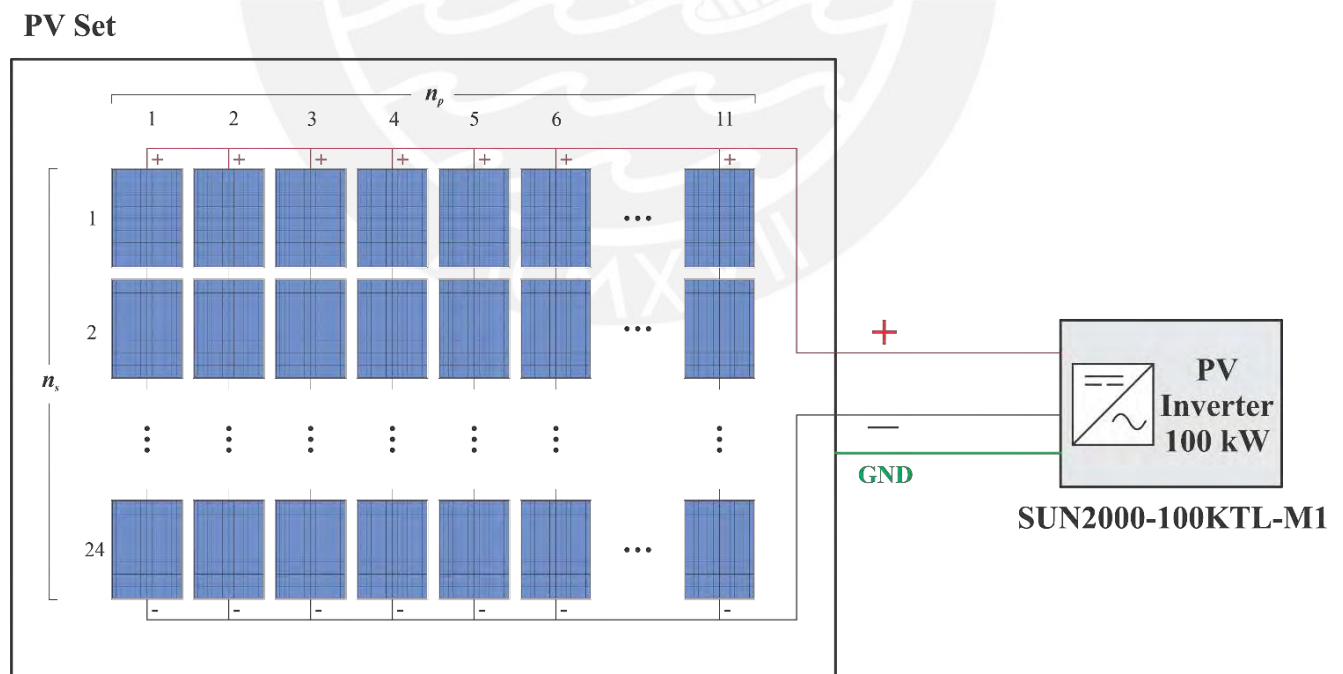


Figure 28: Configuration of a PV station with $n_i = 1$.

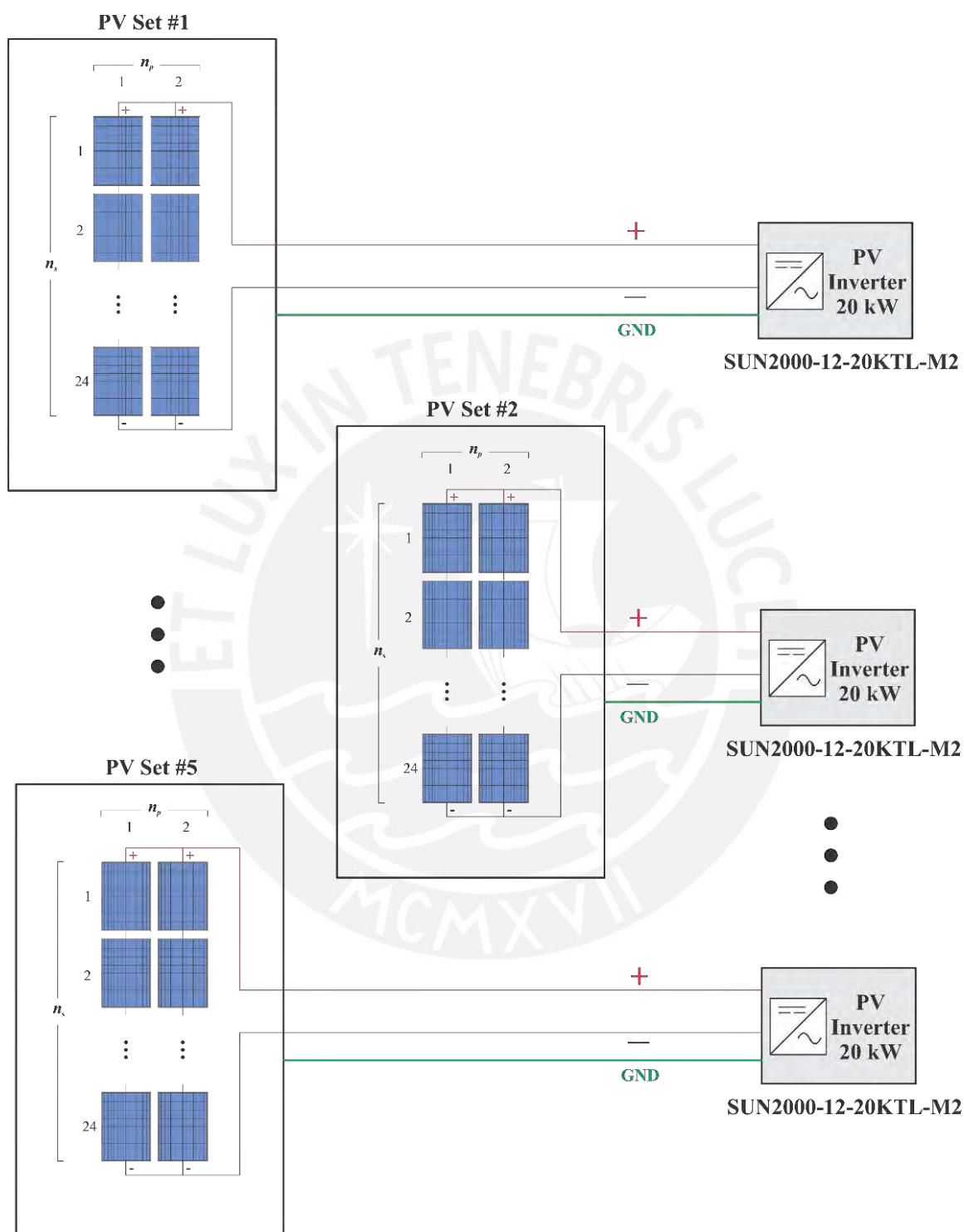


Figure 29: Configuration of a PV station with $n_i = 5$.

4.2 Results and Discussion

Table 10 and Table 11 presents the results obtained by calculating different PV station configurations according to the type and number of PV inverters. It is seen that when the inverter size increases, the failure and repair rate of PV inverters increases and decreases, respectively. In addition, NSEE increases as fewer inverters are used, this is because the failure probabilities are higher when there are fewer transition states in the Markov model for reliability assessment. The analysis and comparison of ELCOE considering different costs and locations is presented below.

n_i	x [kW]	$C(x)$ 2012 [USD]	$C(x)$ 2022 [USD]	λ	μ	n_s	n_p
1	100	43660	15160	0.2032	0.0286	24	11
2	50	233475	9100	0.0803	0.1429	24	6
3	30	14578.5	6030	0.0469	0.1429	24	4
4	25	12324.1	5200	0.0401	0.1429	24	3
5	20	10044	4344	0.0339	0.5000	24	3
6	15	7737.94	3463	0.0283	0.5000	24	2

Table 10: Summary of PV station results (1).

n_i	x [kW]	NSEE [kWh/1-day]	$h = 2.4$		$h = 6$	
			ELCOE 2012 [\$/kWh]	ELCOE 2022 [\$/kWh]	ELCOE 2012 [\$/kWh]	ELCOE 2022 [\$/kWh]
1	100	7363.60	16.35	7.83	6.54	3.13
2	50	727.67	2.21	0.94	0.88	0.37
3	30	516.48	1.85	0.85	0.74	0.34
4	25	582.53	1.93	0.92	0.77	0.47
5	20	38.99	0.91	0.39	0.36	0.15
6	15	30.25	0.91	0.41	0.36	0.16

Table 11: Summary of PV station results (2).

Figure 30 shows the inverter size as a function of the number of inverters. It is clear that the inverter size decays exponentially with the number of inverters in order to, at least, match the maximum required power of the PV station, that is, 86 kWp. For example, at $n_i = 3$ we have $3 \times 30 \text{ kW} = 90 \text{ kW} \geq 86 \text{ kWp}$. The used set of PV inverters in this work are based on the available commercial sizes [39] [40] [41] [42].

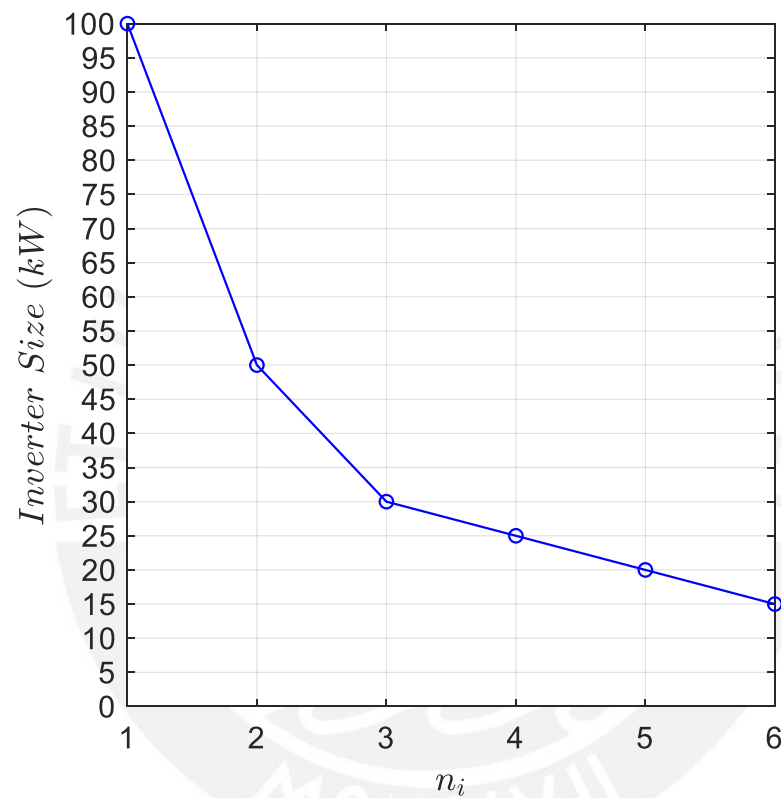


Figure 30: The inverter size as a function of the number of inverters.

The failure rate (λ) as a function of the inverter size is shown in Figure 31. As shown above, λ depends on many factors. The values of λ are calculated based on [2]. Here, the highest value of λ is almost 0.2 for the highest inverter size. This is because higher inverter power losses will lead to higher temperature, and consequently, to higher failure rate as shown in the mathematical equations above.

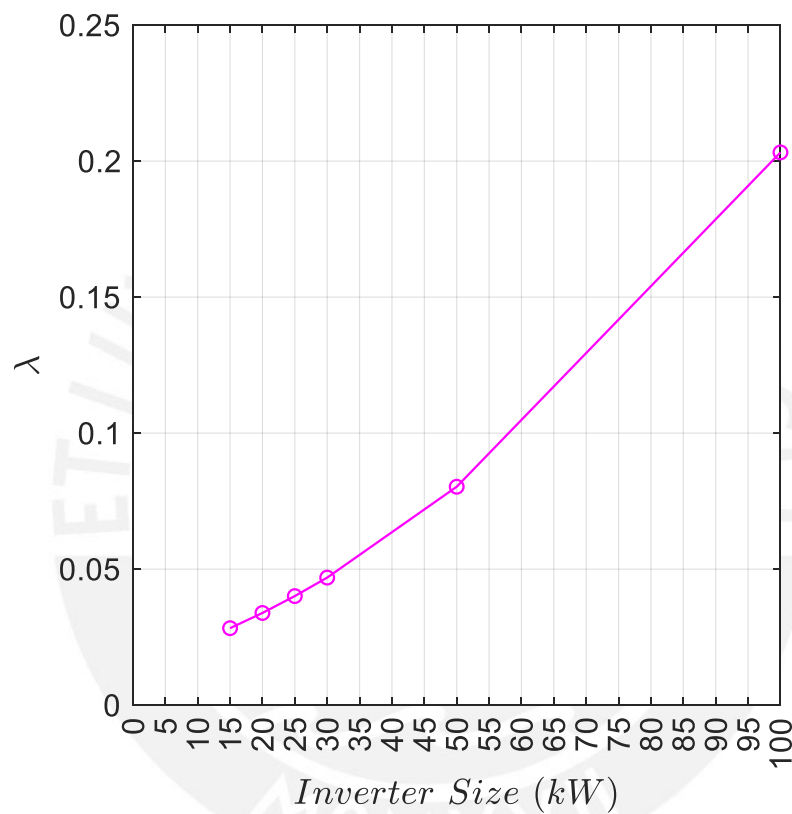


Figure 31: Failure rate (λ) as a function of the inverter size.

Similarly, Figure 32 shows the repair rate (μ) as a function of the inverter size. As explained above, μ depends directly on the size of the inverter. The values of μ have been calculated and adapted from [2] in order to avoid inconsistencies in the calculation of the states of the Markov model. In this case, the lowest value of μ that is below 0.1 belongs to the highest value of the inverter size. This is because the mean time to repair (MTTR) is longer for higher inverter sizes.

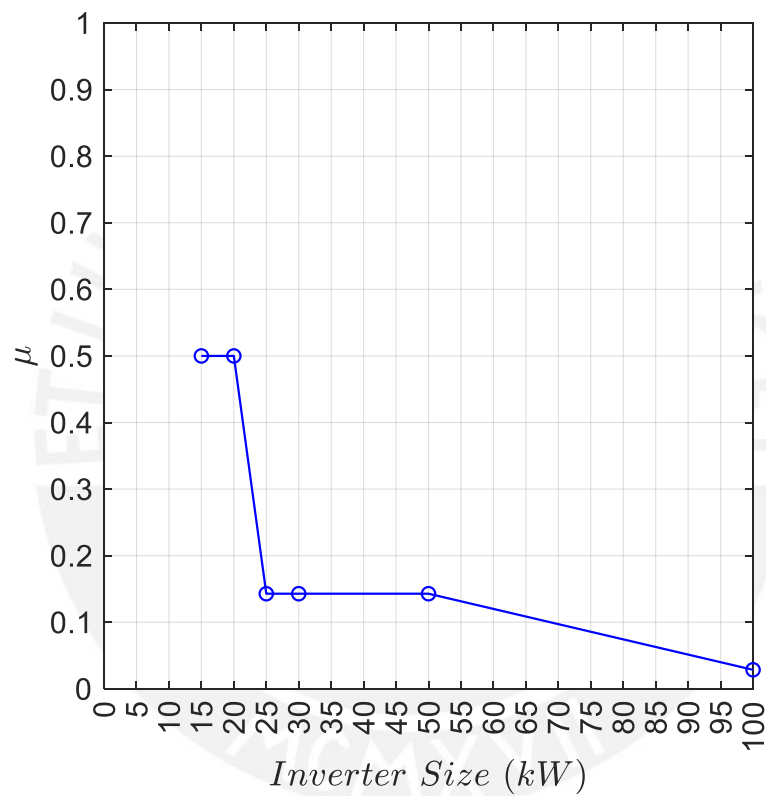


Figure 32: Repair rate (μ) as a function of the inverter size.

Figure 33 shows the NSEE as a function of the inverter size. It can be seen that when the inverter size is large, there is more energy not supplied to the plant. In general, NSEE depends directly on the state probabilities in the Markov model, the size of the inverter and the average time the modules generate power during a year, as shown above. For example, the values of NSEE are almost the same for the inverters with 15 and 20 kW and they increase to almost the same values for the inverters with 25 and 30 kW. This is because the sizes are near to each other. Therefore, there is a big difference between the values for the inverters with 50 and 100 kW. The reason for the highest value at 100 kW is because of using only one large inverter. In this case, if it fails, there will be no generated electricity during the whole failure period in comparison to the other cases.

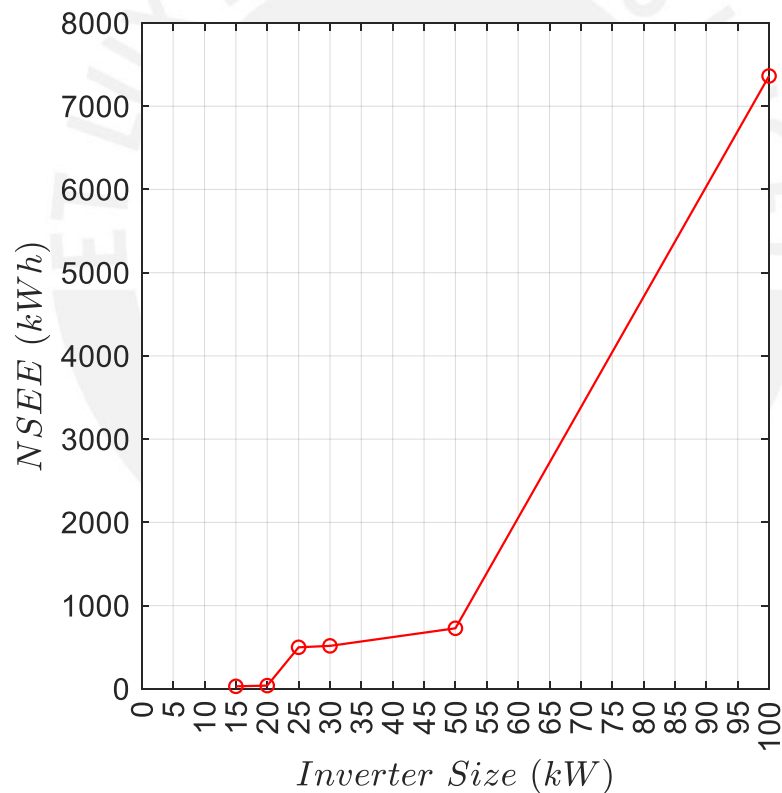


Figure 33: NSEE as a function of the inverter size.

Figure 34 shows ELCOE as a function of the number of inverters considering the prices in 2022. $h = 2.4$ as calculated in the previous chapter with real data from a PV station. In comparison to Figure 33, we found two interesting points. The first point at $n_i = 3$, where a local optimal solution is found. The second point at $n_i = 5$, where a global optimal solution is found in the given search domain. This is because the ELCOE depends not only on the probabilities as in the case of NSEE, but also on the costs of the inverters and their corresponding maintenance and repair cost. Note that the difference between the solutions at $n_i = 5$ and $n_i = 6$ is not so high, 0.39 and 0.41 USD, respectively.

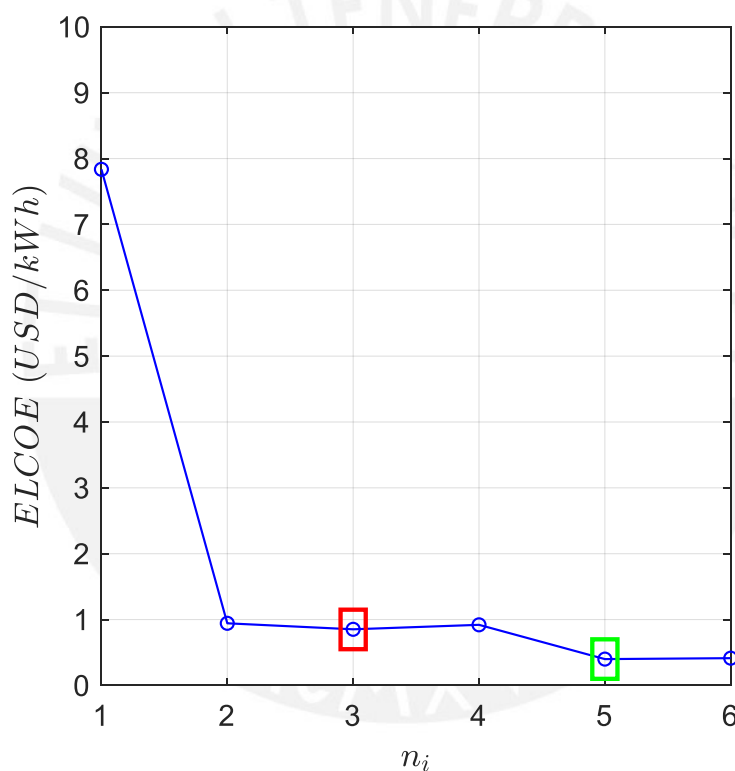


Figure 34: ELCOE as a function of the number of inverters considering the prices in 2022.

Figure 35 shows ELCOE as a function of the number of inverters considering the prices in 2012. $h = 2.4$ as calculated in the previous chapter with real data from a PV station. In this case, the same trend is obtained where the local minimum and global minimum are at $n_i = 3$ and $n_i = 5$, respectively. However, for each case ELCOE values of almost double are obtained according to the results in Figure 34. This is due to the fact that the price of PV inverters was higher 10 years ago. Also, the technology was lower, leading to a higher probability of component failure and an increase in NSEE. For example, the solutions at $n_i = 3$ and $n_i = 5$ are 1.85 and 0.91 USD, respectively.

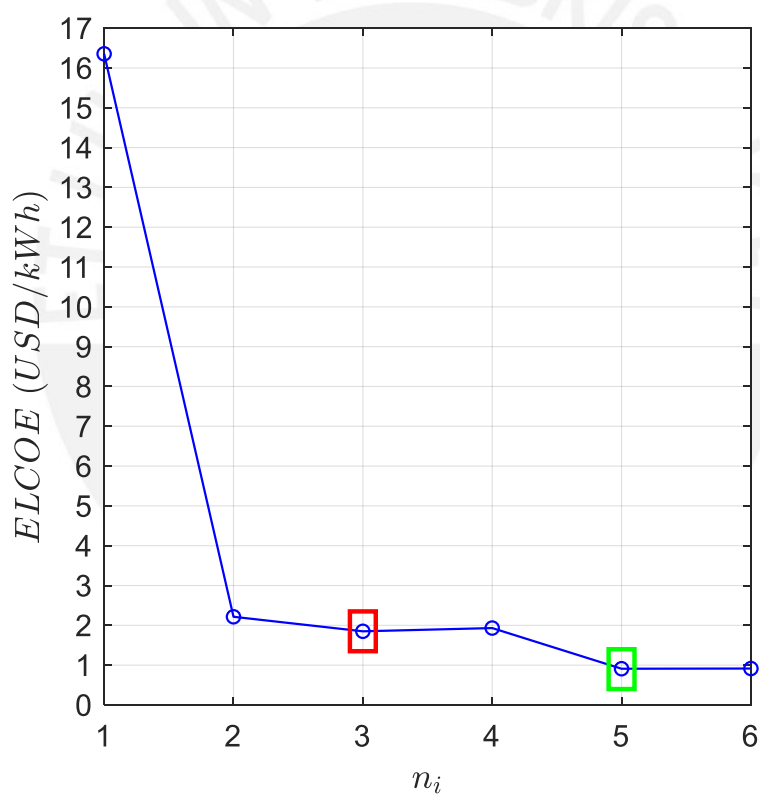


Figure 35: ELCOE as a function of the number of inverters considering the prices in 2012.

Figure 36 shows ELCOE as a function of the number of inverters considering the prices in 2012 and $h = 6$ as presented in [2]. This analysis shows the same trend as in the previous case, where the local minimum and global minimum are at $n_i = 3$ and $n_i = 5$, respectively. However, the effect of the value of h on the result is evident. Lower ELCOE values of almost half are obtained with respect to Figure 35. This is because, greater average sunshine time, higher is the energy produced by the PV modules and, therefore, higher efficiency for the PV plant.

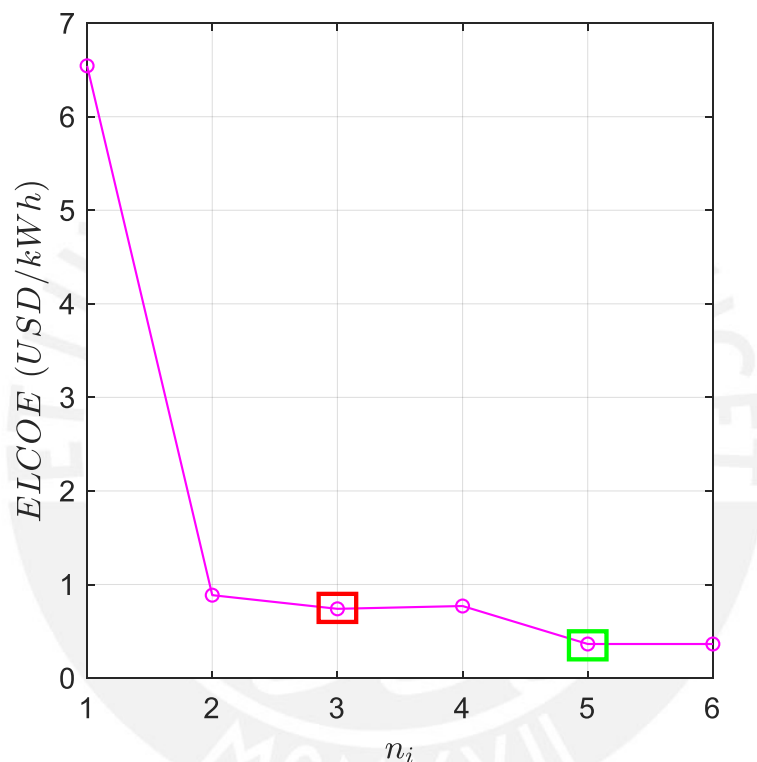


Figure 36: ELCOE as a function of the number of inverters considering the prices in 2012 and $h = 6$.

Figure 37 shows ELCOE as a function of the number of inverters considering the prices in 2022 and $h = 6$ as presented in [2]. Similar to Figure 36, the trend is the same, only that in addition, with current PV inverter prices and with longer sunshine time, the optimal ELCOE value is below 0.2 USD/kWh for PV stations with $n_i = 5$.

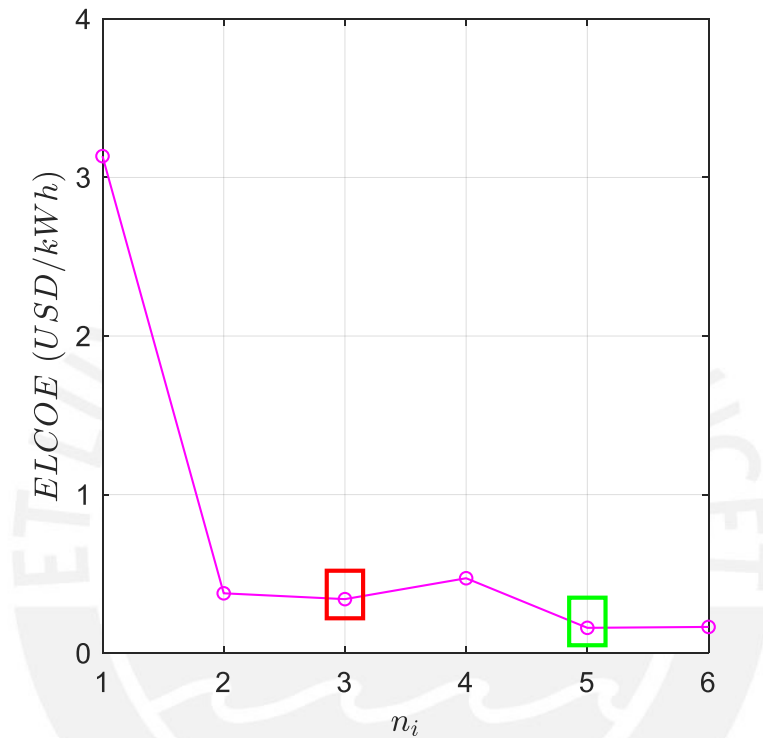


Figure 37: ELCOE as a function of the number of inverters considering the prices in 2022 and $h = 6$.

Chapter 5: Conclusions and Future Work

5.1 Conclusions

In this thesis, we address the problem of energy due the use of conventional sources with a study based on renewable sources such as PV systems. One of the contributions of this master's thesis is to obtain, based on previous studies, a new method to calculate the variables of interest that have a direct effect on the design of a PV station. For this purpose, current and real data of the components that compose a PV system are considered.

Since the main objective is to obtain an optimal design of a PV station, it was necessary to first make calculations of the existing methods and adapt them to the current conditions. Then we studied the behavior of the main component of the PV system: PV inverters. Using the Markov model, an estimation of how the PV system behaves through time is made. A new energy price model is also developed that considers the current costs of the PV inverters. The combination of both methods, the use of real data from a reference PV station and current commercial data makes the difference with respect to previous works.

From an experimental point of view, the main contribution lies in the comparison within different PV station configurations, both in terms of geographical location and the change in PV inverter costs. The results show that the method obtains better results and converges to an optimal solution in terms of ELCOE for PV stations up to 100 kW.

5.2 Future Work

In this thesis, we focus on the evaluation of PV inverters as the main role in the optimal design of a PV station. However, new findings for this study can be considered in the future, such as, for example, contemplating the behavior of PV modules or power transformers to estimate the lifetime of the system and cost-effectiveness. Future work concerns deeper analysis of particular components and new proposals to try different methods to motivate companies in new schemes on sustainable energy generation.

References

- [1] W. Mackenzie, "Solar Market Insight Report 2022 Q3," 2022.
- [2] Z. Moradi-Shahrbabak, A. Tabesh and G. R. Yousefi, "Economical design of utility-scale photovoltaic power plants with optimum availability," *IEEE Trans. Ind. Electron.*, vol. 61, no. 7, pp. 3399-3406, July 2014.
- [3] R. Tidball, J. Bluestein, N. Rodriguez and S. Knoke, "Cost and Performance Assumptions for Modeling Electricity Generation Technologies," *Nat. Renew. Energy Lab. (NREL)*, Golden, Tech. Rep., CO, USA, 2010.
- [4] S. V. Dhople, A. Davoudi, P. L. Chapman and A. D. Domínguez-García, "Integrating Photovoltaic Inverter Reliability into Energy Yield Estimation with Markov Models," in *Proc. IEEE 12th Workshop COMPEL*, pp. 1–5., 2010.
- [5] M. Theristis and I. A. Papazoglou, "Markovian Reliability Analysis of Standalone Photovoltaic Systems Incorporating Repairs," *IEEE Journal of Photovoltaics*. Vol. 4, no. 1, pp. 414-422, 2014.
- [6] MATLAB 2021b, The MathWorks Inc., Natick, Massachusetts, USA.
- [7] C. F. Kutscher, J. B. Millford and F. Kreith, *Principles of Sustainable Energy Systems, Mechanical and Aerospace Engineering Series (Third ed.)*. CRC Press. ISBN 978-0-429-93916-7., 2019.
- [8] M. Roser, "The World's Energy Problem," *Our World in Data*.
<https://ourworldindata.org/worlds-energy-problem>, 2021.
- [9] Geological Survey Ireland, "Fossil fuels," <https://www.gsi.ie/en-ie/education/earth-resources/Pages/Fossil-fuels.aspx>, 2021.
- [10] Global Carbon Project, "Global Carbon Budget 2021: Emissions,"
<https://www.globalcarbonproject.org/carbonbudget/21/infographics.htm>, 2021.
- [11] Twenergy, "Ventajas de la energía nuclear," <https://twenergy.com/energia/energia-nuclear/ventajas-de-la-energia-nuclear/>, 2019.

- [12] M. Roser, "Why did renewables become so cheap so fast?," Our World in Data. <https://ourworldindata.org/cheap-renewables-growth>, 2020.
- [13] Renewable Energy Market Update 2021, "Renewable electricity / Renewables deployment geared up in 2020, establishing a "new normal" for capacity additions in 2021 and 2022.," IEA.org. International Energy Agency., 2021.
- [14] IRENA (2022), "Renewable Energy Statistics 2022," The International Renewable Energy Agency, Abu Dhabi, 2022.
- [15] P. Gevorkian, Large-Scale Solar Power System Design: An Engineering Guide for Grid-Connected Solar Power Generation, McGraw Hill Companies, 2011.
- [16] RSC, "Energy," Royal Society of Chemistry. <https://www.rsc.org/>, 2014.
- [17] B. Norton, "Harnessing solar heat," Springer, Dordrecht, 2014.
- [18] "How CSP Works: Tower, Trough, Fresnel or Dish," SolarPACES. <https://www.solarpaces.org/how-csp-works/>, 2018.
- [19] A. Gando, D. A. Dwyer, R. D. McKeown and C. Zhang, "Partial radiogenic heat model for Earth revealed by geoneutrino measurements," Nature Geoscience, 2011.
- [20] "Biomass Energy Center," Biomassenergycentre.org.uk., 2012.
- [21] J. Marsh, "Monocrystalline and polycrystalline solar panels: which is the best for you?," Energysage. <https://news.energysage.com/monocrystalline-vs-polycrystalline-solar/>, 2022.
- [22] "Comprehensive Guide to Solar Panel Types," Aurorasolar. <https://aurorasolar.com/>, 2022.
- [23] "Tipos de paneles solares," Ecofener. <https://ecofener.com/>, 2019.
- [24] T. Kerekes, E. Koutroulis, D. Séra, R. Teodorescu and M. Katsanevakis, "An optimization method for designing large PV plants," IEEE J. Photovoltaics, vol. 3, no. 2, pp. 814-822, April 2013.
- [25] K. Zipp, "What Is A Solar Transformer?," Solar Power World. <https://www.solarpowerworldonline.com/>, 2013.
- [26] "PV System Types and Components," PennState. AE 868 Commercial Solar Electric Systems. <https://www.e-education.psu.edu/>, 2020.

- [27] Y. Lin, "What are the Differences Between Residential and Commercial Solar?," Energy Link LLC. <https://goenergylink.com/>, 2019.
- [28] "Solar Energy Industries Association," Solar Energy Industries Association. All Rights Reserved., Washington D.C. USA, 2022.
- [29] "National Renewable Energy Laboratory," NREL Transforming ENERGY. U.S. Department of Energy. <https://www.nrel.gov/>.
- [30] Team Clearloop, "What's the difference between Utility-Scale and Rooftop Solar Projects?," Clearloop. A Silicon Ranch Company. <https://clearloop.us/>, USA, 2020.
- [31] L. Rodríguez, "Breaking down growth and perspectives of solar energy: utility, commercial and residential," Rated Power. <https://ratedpower.com/>, Madrid, Spain, 2021.
- [32] "Commercial Solar Panel Systems," Global Point Energy. <https://www.globalpointenergy.ca/>, Canada.
- [33] "Solar Park Pflege," Andreas Lange & Michel GBR. Pfarrgasse 83, 06556 Kalbsrieth. <https://solarparkpflege.de/>, Germany, 2022.
- [34] A. Kornelakis and E. Koutroulis, "Methodology for the design optimization and the economic analysis of a grid-connected photovoltaic systems," IET Renew. Power Gener., Vol. 3, Iss. 4, pp. 476-492, 2009.
- [35] J. D. Mondol, Y. G. Yohanis and B. Norton, "The impact of array inclination and orientation on the performance of a grid-connected photovoltaic system," Renew. Energy, 2007, 32, pp. 118–140, 2007.
- [36] M. Z. Jacobson and V. Jadhav, "World estimates of PV optimal tilt angles and ratios of sunlight incident upon tilted and tracked PV panels relative to horizontal panels," Solar Energy 169 (2018) 55-66. Department of Civil and Environmental Engineering, Stanford University, Stanford, CA 94305-4020, USA, 2018.
- [37] R. Billinton and R. Allan, Reliability Evaluation of Engineering Systems - Concepts and Techniques, New York, NY, USA: Plenum Press, 1992.
- [38] Eco Green Energy, "Solar Panels Poly 72 Cells EOS 330W-350W," datasheet. www.eco-greenenergy.com, France, 2018.

- [39] HUAWEI, "Smart String Inverter SUN2000-12/15/17/20KTL-M2," datasheet Version Nr. 03-(20200528). SOLAR.HUAWEI.COM/DE/, 2019.
- [40] HUAWEI, "Smart String Inverter SUN2000-30/36/40KTL-M3," datasheet. SOLAR.HUAWEI.COM, 2019.
- [41] HUAWEI, "Smart String Inverter SUN2000-(50KTL, 60KTL, 65KTL)-M0," datasheet. SOLAR.HUAWEI.COM/EU/, 2021.
- [42] HUAWEI, "Smart PV Controller SUN2000-100KTL-M1," datasheet. Version No.:04-(20201006). SOLAR.HUAWEI.COM/EU/, 2019.
- [43] Y. A. Shardt, "Statistics for Chemical and Process Engineers: A Modern Approach," Springer International Publishing: Cham, Switzerland. (414 pp.) ISBN: 978-3-319-21508-2., 2015.
- [44] R. Billinton and R. N. Allan, Reliability Evaluation of Power Systems, New York: 2nd ed. Springer/Plenum Press, 1996.
- [45] D. Feldman, G. Barbose, R. Margolis, T. James, S. Weaver, N. Darghouth, R. Fu, C. Davidson, S. Booth and R. Wiser, "Photovoltaic System Pricing Trends - Historical, Recent, and Near-Term Projections 2014 Edition," SunShot U.S. Department of Energy, NREL/PR-6A20-62558, 2014.
- [46] Fraunhofer ISE (2015), "Current and Future Cost of Photovoltaics. Long-term Scenarios for Market Development, System Prices and LCOE of Utility-Scale PV Systems. Study on behalf of Agora Energiewende.," Agora Energiewende, 059/01-S-2015/EN, Berlin, Germany, 2015.
- [47] Fraunhofer ISE, Photovoltaics Report, updated: 22 September 2022, Freiburg, Germany.
- [48] 217F, "Reliability Prediction of Electronic Equipment," MIL-HDBK. Military Handbook, Washington, DC, USA, 1991.
- [49] D. Hirschmann, D. Tissen, S. Schröder and R. W. De Doncker, "Reliability prediction for inverters in hybrid electrical vehicles," IEEE Trans. Power Electron., vol. 22, no. 6, pp. 2511-2517, 2007.
- [50] P. Szabó, O. Steffens, M. Lenz and G. Farkas, "Transient Junction-to-Case Thermal Resistance Measurement Methodology of High Accuracy and High Repeatability,"

IEEE Transactions on Components and Packaging Technologies, Vol. 28, No. 4,
630-636, 2005.



Appendix I: MATLAB Code

I.1 Sub-Code 1: Energy Price Modelling

```
c1_1kw_inv = 1140;           % Cost of 1 kW inverter in 2012
c2_1kw_inv = c1_1kw_inv / 4; % Cost of 1 kW inverter in 2022
c3_1kw_inv = 600;           % Initial cost factor of 1 kW inverter in 2022

c_factor_1 = c1_1kw_inv - c2_1kw_inv;
c_factor_2 = 3;

x_max = 100;
C1 = zeros(1,x_max);
C2 = zeros(1,x_max);
x = 1:x_max;

for i = 1:x_max
    if i==1
        C1(i) = c1_1kw_inv * i;
        C2(i) = c2_1kw_inv * i + c3_1kw_inv;
    else
        C1(i) = 660 + 480 * i - 0.55 * i^2 + 0.0005 * i^3;
        C2(i) = C1(i) - (c_factor_1 * i/c_factor_2);
    end
end
```

I.2 Sub-Code 2: Markov Modelling

```

ni      = 5;          % The required number of inverters
lambda = 0.0339;    % 0.0339 failure/1-year --> For example: lambda = 0.0001142
failures/hr (1 failure/year)
Mu      = 0.5;      % 0.5 repair/1-year --> For example: Mu      = 0.125
restoration/hour

% A: Stochastic transitional probability matrix of ni+1 x ni+1
A = zeros(ni+1,ni+1);

for i=1:(ni+1)
    for j=1:(ni+1)
        if i==1 && j==1
            A(i,j)= 1 - ni*lambda;
        end
        if (i==j) && (i~=1) && (j~=1) && (i~=(ni+1)) && (j~=(ni+1))
            A(i,j)= 1-Mu-(ni-(j-1))*lambda;
        end
        if i==(j-1)
            A(i,j)= (ni-(j-2))*lambda;
        end
        if i==(j+1)
            A(i,j)= Mu;
        end
        if i==ni+1 && j==ni+1
            A(i,j)= 1 - Mu;
        end
    end
end
end

```